BY

MULUGETA MILKIAS

AASTU, 2021

ADDIS ABABA SCIENCE AND TECHNOLOGY UNIVERSITY

GEOCHEMICAL INSIGHT ON GEM OPAL FORMATION IH HIGHLY WEATHERED RHYOLITIC IGNIMBRITE LAYER FROM DELANTA AREA, SOUTH WOLLO, NORTHERN ETHIOPIA

A MASTER THESIS

BY

MULUGETA MILKIAS

TO

DEPARTMENT OF GEOLOGY

APPLIED SCIENCE COLLEGE

AUGUST, 2021

ADDIS ABABA SCIENCE AND TECHNOLOGY UNIVERSITY

GEOCHEMICAL INSIGHT ON GEM OPAL FORMATION IN HIGHLY WEATHERED RHYOLITIC IGNIMBRITE LAYER FROM DELANTA AREA, SOUTH WOLLO, NORTHERN ETHIOPIA

By

MULUGETA MILKIAS

ADVISORS: TESFAYE DEMISSIE (Assi. Professor**)**
DANIEL MESHESHA (Assi. Professor**)**

A Thesis Submitted as Partial Fulfilment of the Requirements for the award of Degree of Master of Science in Geology (Economic Geology)

To

DEPARTMENT OF GEOLOGY

COLLEGE OF APPLIED SCIENCE

AUGUST, 2021

Declaration

I hereby declare that this thesis entitled **"Geochemical insight on gem opal formation in highly weathered rhyolitic ignimbrite layer from Delanta area, south Wollo, northern Ethiopia"** was prepared by me, with the guidance of my advisors Dr. Tesfaye Demissie and Dr. Daniel Meshesha. The work contained herein is my own except where explicitly stated otherwise in the text, and that this work has not been submitted, in whole or in part, for any other degree or professional qualification.

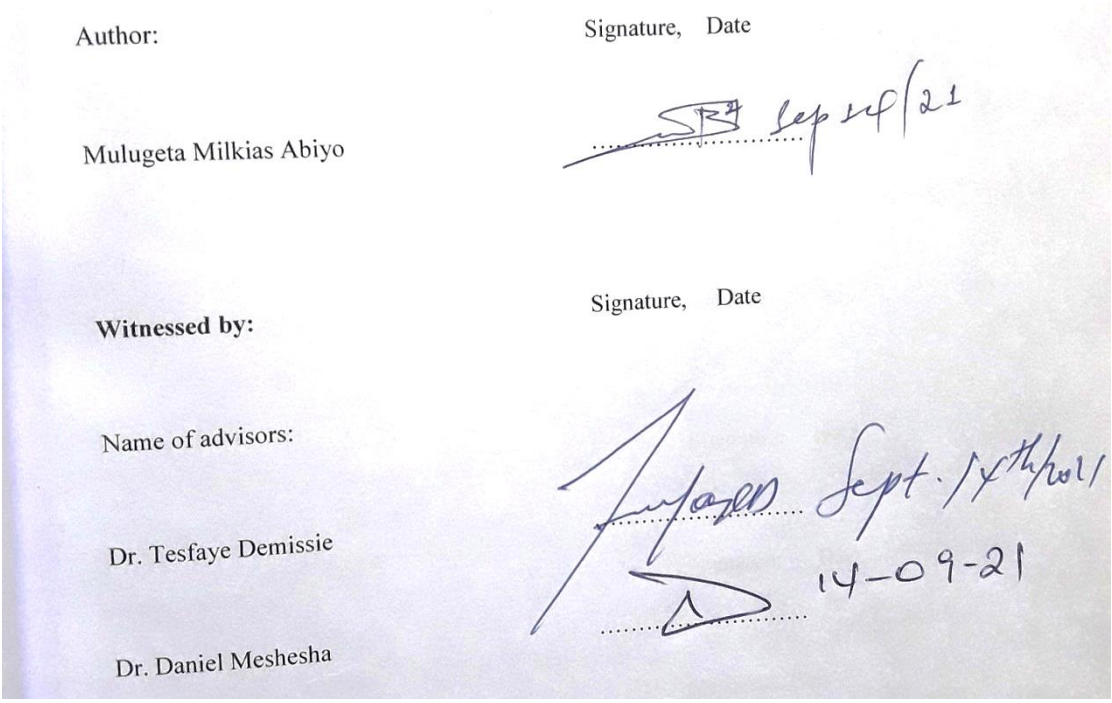

Certification

This is to certify that the thesis prepared by **Mr. Mulugeta Milkias** entitled "**Geochemical insight on gem opal formation in highly weathered rhyolitic ignimbrite layer from Delanta area, south Wollo, northern Ethiopia"** and submitted as partial fulfilment for the Award of the Degree of Master of Science complies with the regulations of Addis Ababa Science and Technology University and meets the accepted standards concerning the originality, content, and quality.

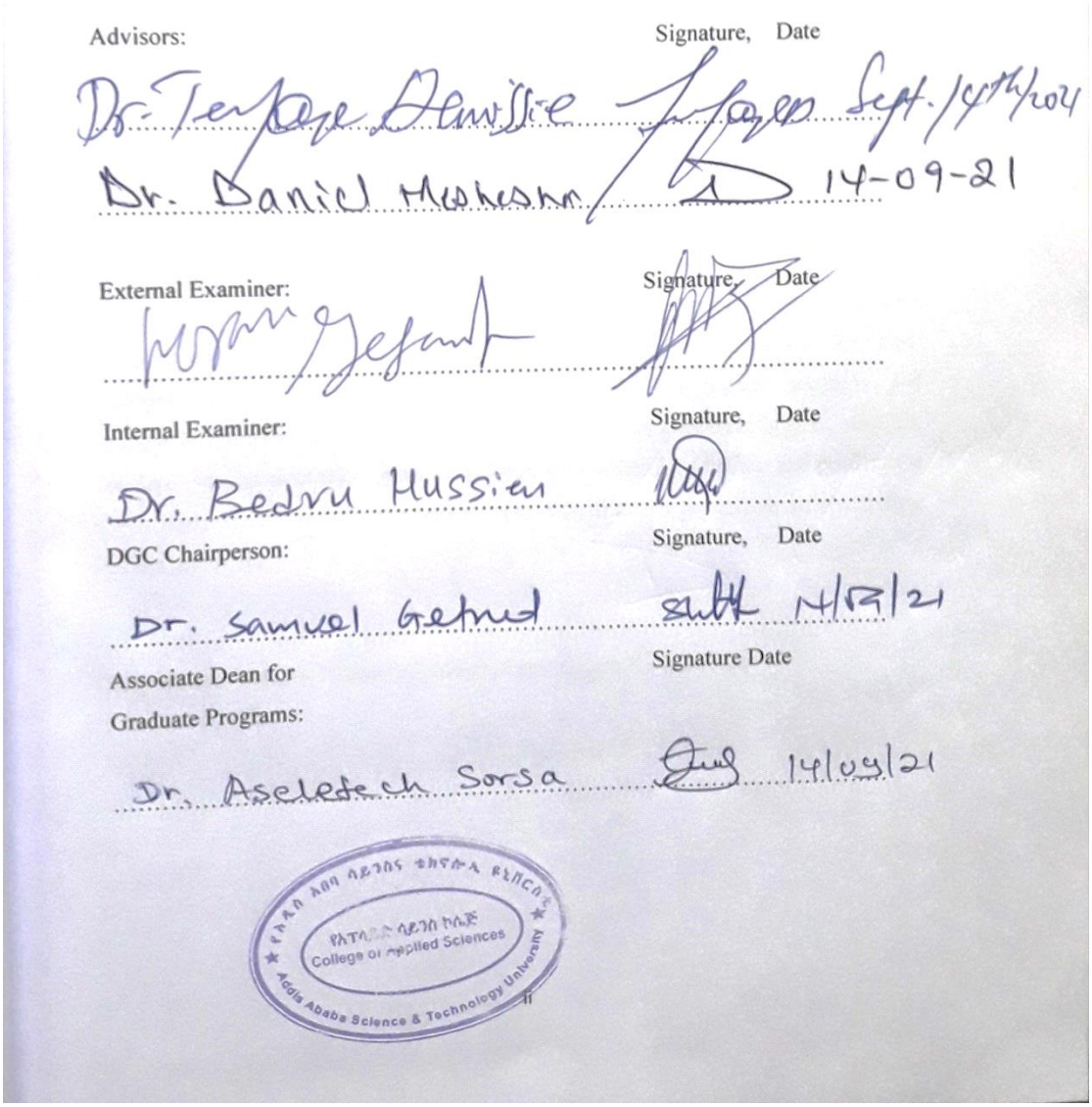

Abstract

A gem-quality opal is found in Delanta Woreda especially in Wegel Tena, and Tsehay Mewucha locality. The region consists of a thick (>3,000 m) volcanic sequence of basalt and rhyolitic ignimbrite. Over this volcanic series, only one very thin layer (<3 m thick), of rhyolitic ignimbrite is mineralized with opal. The main objectives of this study were understanding the relationship between opal with its host rock and propose genetic model for opal. It is examined using petrographic description, and whole-rock geochemistry (major and trace element analysis) of the host rhyolitic ignimbrite and opal. To achieve this, samples are directly extracted from three different local mining sites of Delanta area (Tantakoa to the northeast, Worke Washa to the east, and Berbere Wenz to the south of the study are) from the opal bearing layer. Petrographically, the matrix is composed of glassy, non-crystalline, and amorphous groundmass (>75%), occasionally welded and mostly weathered with varying size phenocrysts of quartz, plagioclase, and sanidine. Regarding the result of trace element geochemistry, rhyolitic ignimbrite and opal samples show variable characteristics always a lesser concentration in opal. The presence and concentration of trace elements in opals reflect primarily the host-rock composition, as silica in opal comes from its weathering. The rhyolitic ignimbrite show an almost gentle REE pattern with a more or less pronounced enrichment in LREE compared to HREE. The opal samples show typical depletion from LREE to HREE, Eu negative anomaly, and generally a positive Ce anomaly. Strongly weathered opal-bearing horizon with the presence of abundant clays, granular microstructure, high LOI values, and positive Ce anomaly demonstrates that the Delanta opal formed during an episode of weathering of the host rock.

Key words: Delanta, Northern Ethiopia, Opal, Origin, Comparison

Acknowledgment

For most and above all, I would like to express my gratitude to the **Almighty God**, through who all things are possible and who strengthens me.

Too difficult to do a master's thesis without the assistance and encouragement of other people. At the very outset of this thesis report, I would like to extend my heartfelt thanks to all the personages who have helped me in this endeavor. Without their active guidance, help, cooperation, and encouragement, I would not have made headway in the thesis.

First of all, I am extremely grateful to my advisors Dr. Tesfaye Demissie and Dr. Daniel Meshesha for their relentless, encouragement and advice which was played a pivotal role in the success of this study.

I am extremely grateful to Addis Ababa Science and Technology University for sponsoring my thesis work.

I would like to acknowledge and pay my gratitude to all the staff of the college of Applied Science, Department of eology for their valuable support in the completion of this thesis.

At last but not least gratitude goes to all of my families and friends who directly or indirectly helped me to complete this thesis. Any omission in this brief acknowledgment does not mean a lack of gratitude.

Table of contents

List of figures

List of tables

List of acronyms

AASTU	Addis Ababa Science and Technology University
ALS	Australian Laboratory Services
GPS	Global Positioning System
HREE	Heavy Rare Earth Element
ICP-AES	Inductively Coupled Plasma Atomic Emission Spectroscopy
ICP-MS	Inductively Coupled Plasma Mass Spectroscopy
LOI	Loss on Ignition
LREE	Light Rare Earth Element
PPL	Plane Polarized Light
REE	Rare Earth Element
UTM	Universal Transverse Mercator
XPL	Cross Polarized Light

CHAPTER ONE

1. INTRODUCTION

1.1 BACKGROUND OF THE STUDY

A gemstone or gem also called a precious or semi-precious stone, is a piece of attractive mineral which when cut and polished is used to make jewelry or other adornments (Zewdie et al., 2009). Opal, aquamarine, emerald, peridot, garnet, spinel, tourmaline, topaz, jadeite, sapphire, ruby, amethyst, agate, jasper, etc. are some of the minerals used as a gem (Bobon, 2011). Most gemstones are hard, but some soft minerals or noncrystalline materials of organic origin (e.g., pearl, red coal, and amber) are used in jewelry because of their lustre or other physical properties that have astatic value [(1a)]. Rarity is another characteristic that adds value to a gemstone.

According to Bobon (2011), opal is one of the planet's rarest and most unique gemstones. It is the world's most beautiful, precious, and one of six types of gemstones used throughout history, along with diamonds, rubies, sapphires, emeralds, and pearls. We can purchase any other precious stones such as emerald, ruby, sapphire, or diamond, only to find that their colors all seem similar. With an opal, we are getting a unique pattern that no one else in the world owns. All opals are unique in their character, shade, depth, color, and pattern play with some brighter than others.

There are two broad classes of opal: precious and common (Gaillou et al., 2008). Precious opal displays play-of-color (iridescence), common opal does not. Play-of-color is defined as "a pseudo chromatic optical effect resulting in flashes of colored light from certain minerals, as they are turned in white light." The internal structure of precious opal causes it to diffract light, resulting in play-of-color. Depending on the conditions in which it formed, opal may be transparent, translucent, or opaque and the background color may be white, black, or nearly any color of the visual spectrum (Gaillou et al., 2008).

Gem-quality opals for the most part come from two types of deposits: volcanic and sedimentary (Johnson et al., 1996). It is come from the weathering of silicic rocks, and precipitation from a SiO_2-enriched liquid in cavities (Gaillou et al., 2008). The

1a (https://www.britannica.com/science/gemstone)

host rock for sedimentary and volcanic environment is mostly sandstone and rhyolite respectively.

This study focused on the relationship between opal with its host rock and genesis of opal mineralization in Delanta area. Therefore, our data set has been used to understand the geology and to investigate the relationship between opal and its host rock. It's also intended to outline the geological and geochemical condition which is responsible for opal mineralization. The research will be performed by using petrographic and geochemical analysis of host rock and opal samples which are systematically collected from the study area.

1.2 DESCRIPTION OF THE STUDY AREA

1.2.1 Location and accessibility

The study area is located in Amhara National Regional State in the south Wollo zone, Delanta woreda. It is found ~550 km north of Addis Ababa. The locality has also been referred to as "Delanta," which corresponds to a former subdivision (or "awraja") of Wollo Province. The area is accessible through Addis Ababa – Dessie town main asphalt road, which has ~410km a total length, and also an additional ~140 km gravel road that connects Dessie with the study area. Other small towns in the area are accessible with a four-wheel-drive vehicle and connected with networks of dry weathered roads and these roads are used to access different parts of the study area.

A lot of recently discovered traditional mining sites are distributed in all directions of the stud area. The opal occurs in a horizontal layer that is exposed on a cliff of a canyon. Various mine sites are reached by walking down the steep canyon for more than one hour (Tantakoa, Berbere Wenz, and Worke Washa). The study area is bounded in 1276930m-1293108m N and 515090m-534028m E, and falls in the Ethiopian Mapping Agency topographic map of GISHEN sheet (1139A4, Edition 1 EMA 1996) and WEGELTENA sheet (1139A3, Edition 1 EMA 1996) 1:50,000 scale.

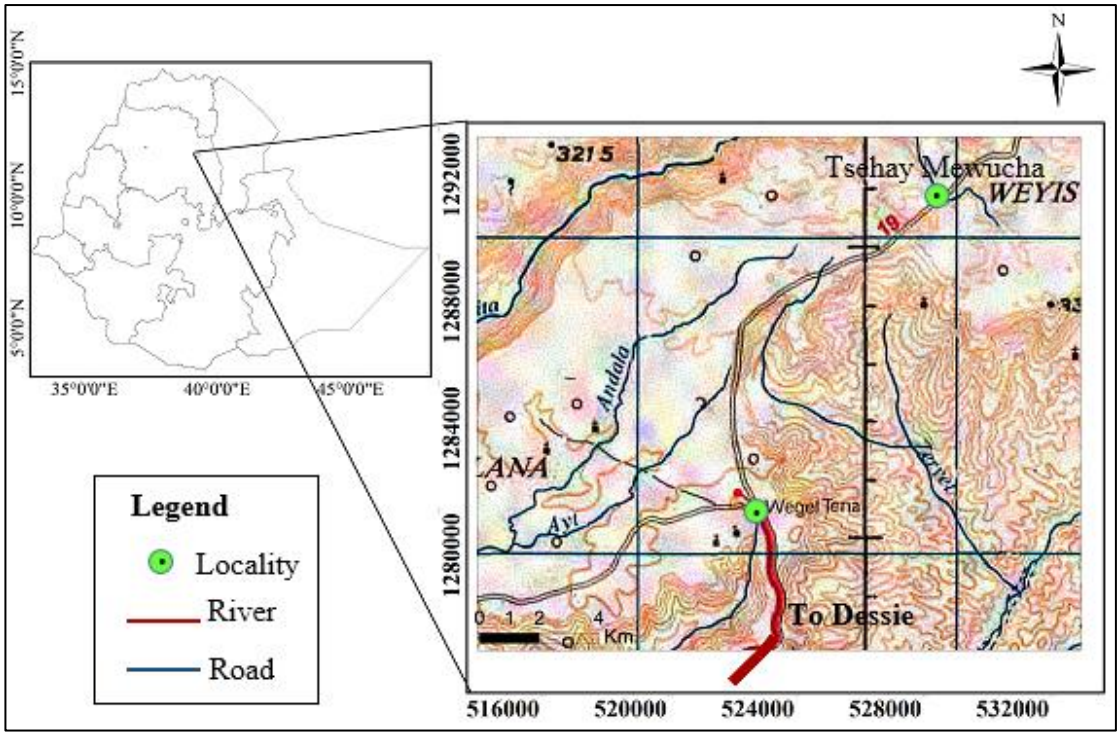

Figure 1. 1: Location map of the study area, Delanta, Wollo province.

1.2.2 Climate

The available nearby metrological station is Kombolcha metrological station. According to the data from this metrological station, the mean annual rainfall and climate of the region range between 614.80mm-968.7 mm, and 5.9 – 19.11^{0}C respectively. The minimum average temperature is 1.6^{0}C in October to 7.1^{0}C in December. Moreover, 21.2^{0}C and 28.0^{0}C are the maximum temperatures recorded in January and June respectively. (Source: Delanta Woreda information bureau).

1.2.3 Physiography and drainage

The study area is characterized by undulating topography with cliffs, valleys, and deep gorges. The altitude ranges from 2400m to 3300m a.s.l. The southern and eastern part of the study area shows small variation in elevation difference that ranges between 2700m and 3000m a.s.l. However wide variation is seen in the northern and northeastern parts which range between 2400m to 3300m a.s.l. The peak 3300m is around Tsehay Mewcha locality in the northeastern part of the study area.

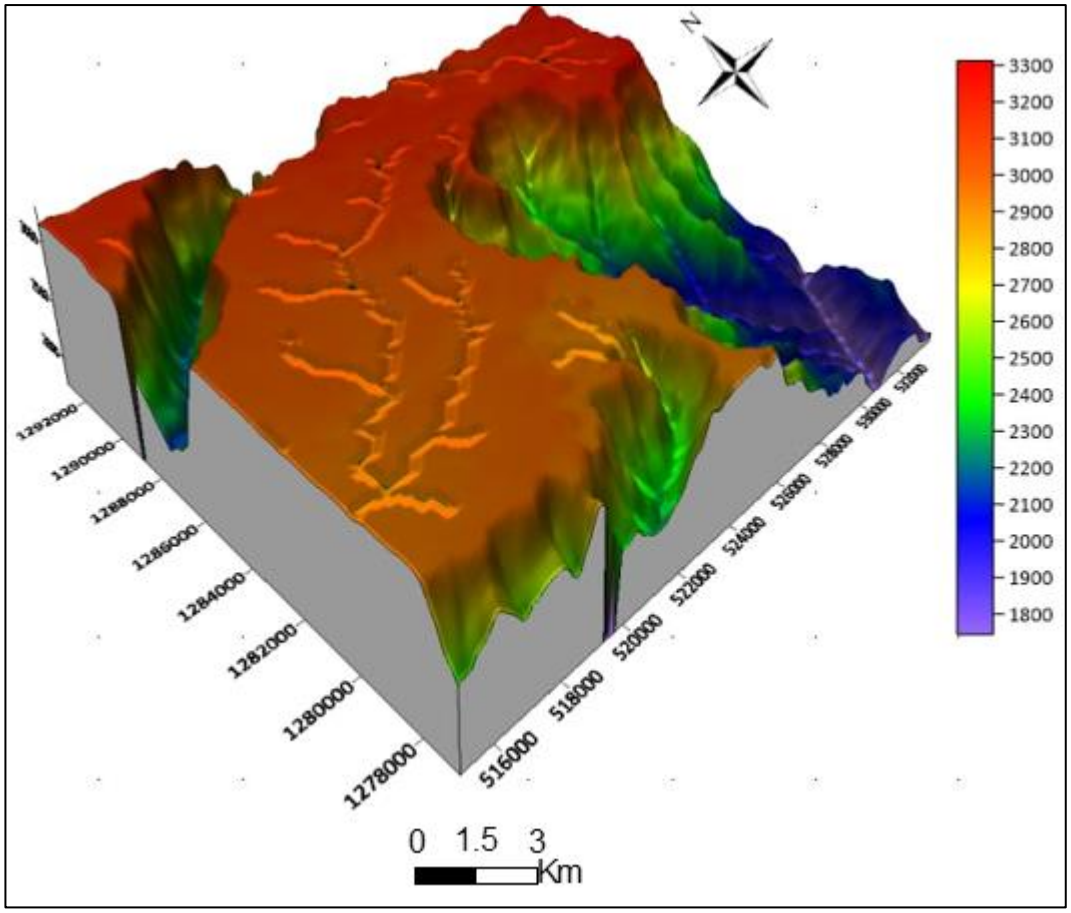

Figure 1. 2: Physiographic map of the study area interpreted from digital elevation model 3-dimensional view.

The drainage network is subparallel to a dendritic pattern. The major rivers show subparallel patterns whereas the tributaries have a dendritic pattern. The major rivers are perennial and they form V shape steep valleys and gorges whereas the tributaries are intermittent. The streams drain from NE to SW and NW to SE.

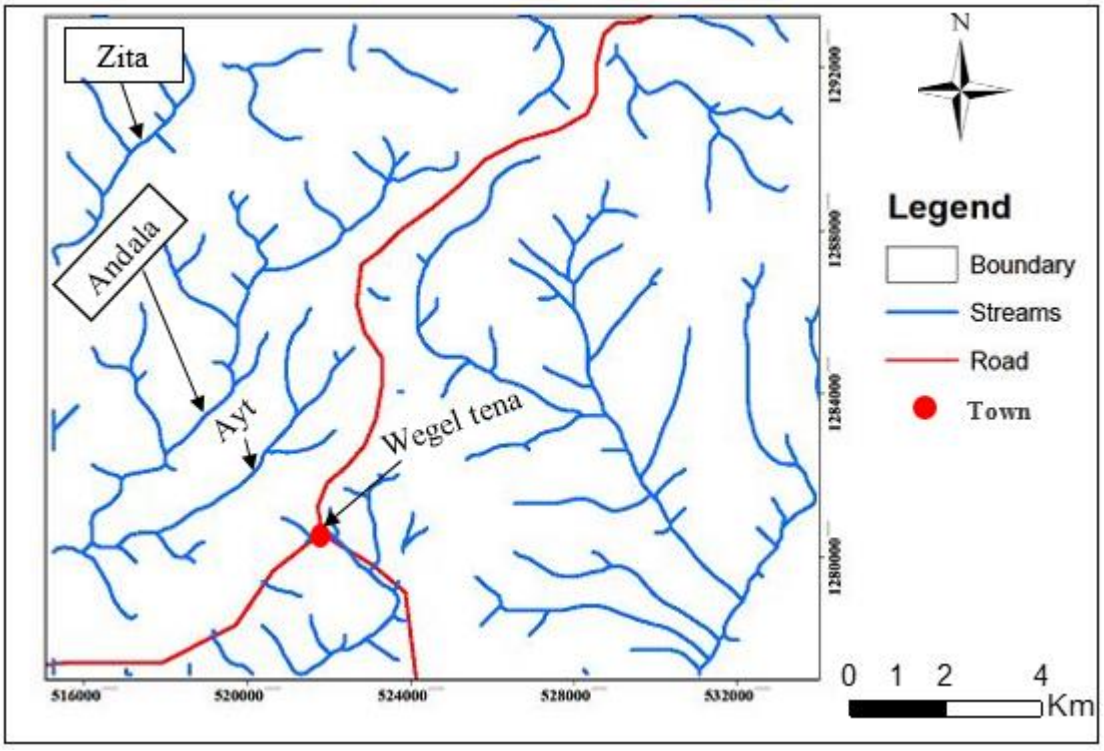

Figure 1. 3: Drainage map of the study area.

1.3 STATEMENT OF THE PROBLEM

From an economic point of view, a better understanding of the condition of a formation may help in developing a guideline for opal exploration (Rondeau et al., 2012). Knowledge on the relationship of opal and its host rock is used to understand geologic processes and their formation. It will increase our ability to develop an exploration model to assist the mining industry (Gaillou et al., 2008).

Chauvire et al. (2019) and Rondeau et al. (2012) described the origin of Wegel Tena opal based on their trace element chemistry. The gap left by the authors is that the relationship between opal mineral and its host rhyolitic ignimbrite is much less constrained. So the required remedy for the existing problem is to fill the gap left by these authors (i.e.to outline the relationship between the host rhyolitic ignimbrite and opal) in the study area and give recommendations for further exploration and exploitation of the resource.

The thesis work comes out with, geochemical characterization of the host rock and opal, to outline the relationship and genesis of opal. The research were done by using petrographic and geochemical analysis of samples which are systematically collected from the host rock and opal mineral of the study area and be a guideline for the

production of opal than the former production capacity.

1.4 OBJECTIVE

1.4.1 General objective

This study is generally intended to understand the geology and characterize the geochemistry of the opal bearing layer, in Delanta area, south Wollo, northern Ethiopia.

1.4.2 Specific objective

The specific objectives of the study were:

- ✓ Conduct petrographic description of the host rock
- ✓ Propose the genetic model for the mineralization
- ✓ Comparison of Delanta opal with some known world opal mineral

1.5 METHODS AND MATERIALS

Beginning from the initial planning to the end of this work, different materials and methods have been used.

1.5.1 Secondary data collection

The following activities were done before the fieldwork have been conducted.

- ✓ Previous data collection: different geological, geochemical, and gemological reports, maps have been collected and compiled with an emphasis on the study area.
- ✓ Before the field work, the study area is delineated using Arc GIS software from a 1:50,000 scale topographic map of Wegel Tena and Gishen sheet and 1:250,000 scale geologic map of the Dessie map sheet.
- ✓ Available information like temperature, rainfall data, forest, and soil coverage, accessibility, and geomorphological setup of the area was compiled from a topographic map, Google Earth, and different existing data.

1.5.2 Sample collection

Different activities were conducted in the field. The first day of the fieldwork involved reconnaissance of the overall geology of the area was outlined and sampling

sites were selected. The other days were spent on the local geology and collection of representative samples for petrographic study and geochemical analysis.

During the field investigation, an attempt was made to describe the geology of the area and opal host rock samples in detail at the hand specimen scale. A sampling of representative host rock and opal samples from the mining sites was one of the fundamental activities that were done during the fieldwork. A total of 25 (18 rhyolitic ignimbrites, and 7 opals) samples from three different artisanal mining sites (Tantakoa area to the northeast, Worke Washa to the East, and Berbere Wenz to the south of the study area) were collected. All of the samples are collected from 50m to 100m long local mining tunnels (6 samples of rhyolitic ignimbrite from each mining site) with megascopic description includes both color and textural variations and then immediately stored in a closed plastic bag. The sample codes have a prefix, starting with the locality name where the samples are collected from.

1.5.3 Laboratory analysis

Thirteen (13) rhyolitic ignimbrite rock samples were sent to the Ethiopian Geological Survey central laboratory for thin-section preparation. The petrographic study was done for the host rock of opal. The thin-sectioned samples were examined using a petrographic microscope in the Addis Ababa Science and Technology University (AASTU) department of the geology petrology laboratory. The petrographic description includes mineralogical and textural characteristics of the samples, and then their results were presented and interpreted.

13 (i.e. 10 rhyolitic ignimbrites and 3 opals) samples were sent to Australian Laboratory Services (ALS), Addis Ababa, Ethiopia. The preparation code for the process is called PREP-31. The samples were crushed into chips with 70% of the crushed samples being less than 2mm in size. Then, the crushed samples were further pulverized up to 250g with 85% of the samples passing through 75 microns, and splitting the samples was done using the riffle splitter. Subsequently, the pulverized samples or pulp weighing 0.7 kg were sent to Ireland and processed at ALS Loughrea, Ireland. The methods and procedures used to process the whole-rock geochemical analysis are presented below.

The methods used for the analysis of major oxides are ICP-AES which is coded as ME-ICP06 and OA-GRA05. Samples are decomposed using lithium metaborate/lithium tetraborate fusion. A prepared sample (0.2 g) is added to lithium metaborate/lithium tetraborate flux (0.90g), mixed well, and fused at 1000^0C. The resulting melt is then cooled and dissolved in 100mL of 4% nitric acid/2% hydrochloric acid. This solution is then analyzed by ICP-AES and the results are corrected for spectral inter-element interferences. Oxide concentration is calculated from the determined elemental concentrations and the result is reported in that format. The total oxide content is determined from the ICP analytic concentrations and loss on ignition (LOI) values. A prepared sample (0.1g) is placed in an oven at 1000^0C for one hour, cooled, and weighed. The percent on loss ignition is then calculated from the difference in weight.

The method used for ultra-trace element analysis is ICP-MS, which is coded as ME-MS81D. The samples are decomposed using lithium metaborate fusion (FUS-LI01). A prepared sample of 0.2g is added to lithium metaborate flux (0.90g), mixed well, and fused in a furnace at 1000^0C. The resulting melt is then cooled and dissolved in 100mL of 4% nitric acid HNO_3/2% HCI (hydrochloric acid). This solution is then analyzed by ICP-MS.

The quality of the analysis was controlled by checking reproducibility and repeatability of the data by using blank, and international rock standards (REE-1 and SY-4).

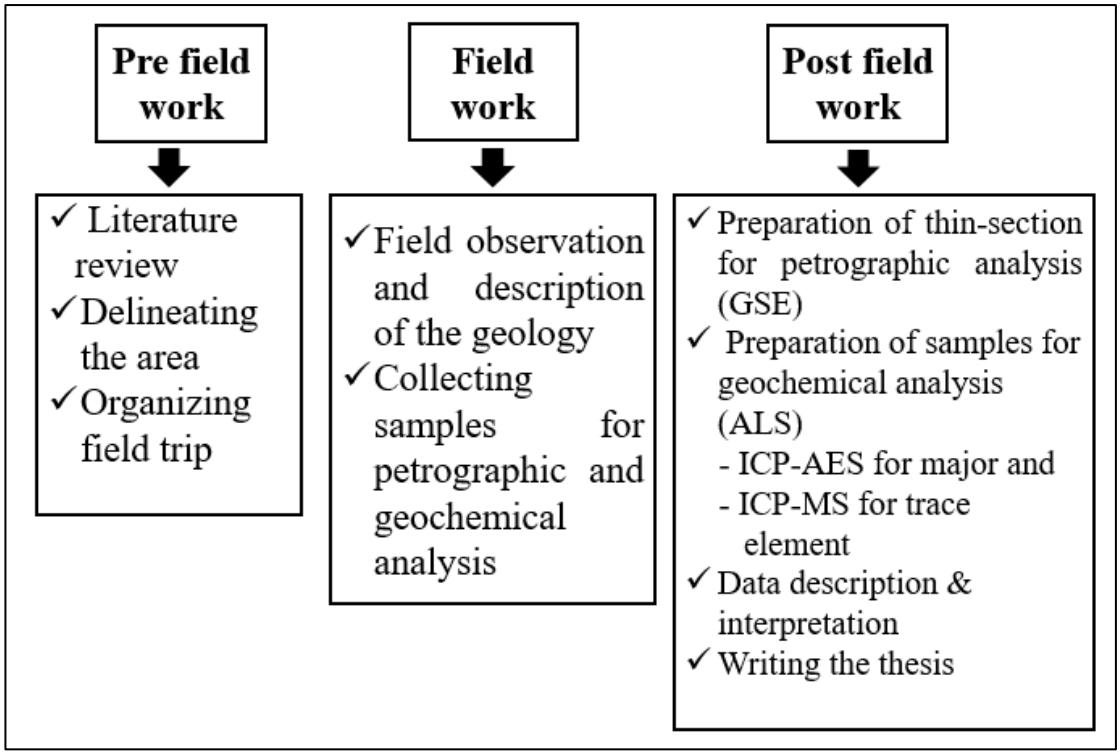

Figure 1. 4: Schematic chart of methodology.

CHAPTER TWO

2. LITERATURE REVIEW

2.1 INTRODUCTION

Opal (chemical formula $SiO_2.nH_2O$) corresponding to a hydrated, amorphous, or poorly crystallized (Gaillou, 2006) and made of closely packed spheres of silica in hexagonal and /or cubic closest packing (Klein et al., 1993). The void between the spheres is occupied by air and water. The water content can vary from 3 to 16% of its weight (Aguilar-Reyes, 2004); hardness is between 5.5-6.5, density can vary from 0.67 for certain hydrophane opals to 2.23 for other varieties (Gaillou, 2006) and its refractive index can vary between 1.42 and 1.475 (Aguilar-Reyes, 2004), Specific gravity variable, 1.8-2.5, and the streak is white. The specific gravity and refractive index decrease with increasing water content (Aguilar-Reyes, 2004).

2.2 ETHIOPIAN OPAL

2.2.1 Discovery

The discovery of opal in Ethiopia date back to 1994 (Johnson et al., 1996). It is reported to occur in central Ethiopia, in Amhara Regional State, Northern Shoa, around Menze and Gishe and Bulga zone, Mezezo (Zewdie et al., 2009). Opals from Shewa Province have near-colorless to white, yellow, orange, or brown body colors; some show face-up play-of-color, and many have contra luz (that is, play-of-color only visible with transmitted light). The gemmological properties are consistent with those of other natural opals, and small particles are common inclusions. The opal-bearing rock is nodular rhyolite (Jonhson et al., 1996).

According to Rondeau et al. (2010), another major discovery was seen in 2008 near the village of Wegel Tena, in volcanic rocks of Wollo province. Unlike previous Ethiopian opals, the new material is mostly white, with some brown opal, fire opal, and colorless “crystal” opal. Some of it resembles Australian and Brazilian sedimentary opals, with play-of-color. The entire region around Wegel Tena consists of a thick (>3,000 m) volcanicano-sedimentary sequence of alternating layers of basalt and rhyolitic ignimbrite. Only one very thin layer (<1 m thick), hosted by ignimbrite, is mineralized with opal. The opals range from opaque to transparent, but

most are translucent. Another behavior observed was that all opaque-to-translucent samples became more transparent when immersed in water for a few minutes to one hour, depending on the thickness of the sample. This behavior is typical of hydrophane characteristics and Play-of-color was commonly distributed along with parallel columns that resembled fingers. They refer to such features as digit patterns.

Another source was discovered in Wollo, at the Stayish mine near the town of Gashena in 2013 (Kiefert et al., 2014). This discovery has yielded mostly dark and black opal, along with some white and crystal opal. It is set in a distinct opal-bearing layer in a mountainous area at an altitude of around 3,000 meters. The black opal is found at the contact zone between the volcanic rock series and the underlying clay-rich layer. The layer is one in a sequence of repeating volcanic ash and ignimbrite layers. The opal-bearing layer is contained in a single stratum extending for tens and even hundreds of kilometers along the mountain belt and it's about 60 cm thick and contains opal of various qualities and colors.

2.2.2 Genesis

Opal forms either in volcanic or sedimentary deposits (Johnson et al., 1996). It is believed to come from the weathering of silicic rocks (rhyolite or sandstones for example), followed by precipitation from a SiO_2-enriched liquid in cavities (Gaillou et al., 2008). Generally, three main formation processes have been identified for opal mineralization which indicates their origin: biological precipitation, hydrothermal alteration, and continental weathering (Chauvire et al., 2019). Opaline silica (biogenic silica) is also a form of biologically produced silicon dioxide (SiO_2. nH_2O) secreted as skeletal material by pelagic phytoplankton (diatoms) and one group of pelagic zooplankton (radiolarians) accumulating in oceanic or lacustrine sediments (Andrews et al., 1996; Iler, 1979; Chauvire et al., 2019). Hydrothermal waters are loaded with chemical substances dissolved from rocks at high temperatures. As long as the water remains hot, the dissolved material can remain in the solution. However, as hydrothermal waters coming to the surface quickly cool and fluids are highly mobile and chemically reactive, making them excellent solvents for silica (SiO_2) bearing rocks and minerals (Jones and Renaut, 2003, 2004). Hydrothermal alteration is involved in amorphous silica precipitation in hot springs (e.g. geysers) and hydrothermal vents (e.g. black smokers) (Chauvire et al., 2019). The alteration as

being when precipitation occurs at a temperature above 50^0C (Pirajno, 2009). However, continental weathering of rocks also dissolves primary minerals and liberates silica available for the formation of secondary minerals, including opal (Chauvire et al., 2019). Weathering when precipitation occurs at a temperature below 50^0C (Pirajno, 2009). During the weathering process, feldspathic tuffs are readily kaolinized and converted to soft earthy masses. One of the earliest changes in vitric tuff is the release of silica and the deposition of hydrated silica –opal and chalcedony that may convert these felsic tuffs to a dense flinty rock very much resembling chert (Chauvire et al., 2019).

There are numerous small deposits of opals around Wegel Tena and Tsehay Mewucha localities. All found at a single stratigraphic level and hence all formed at the same time. This layer belongs to a thick sequence of volcanic ash rich in silica called ignimbrites, forming a volcanic tuff (Rondeau et al., 2011).

The Wegel Tena opal is formed during the Oligocene period (24 to 34 Ma) when volcanic emissions stopped for a long time. This episode had to be long enough to weathering of the host ignimbrite and release the silica. The silica has two origins. The first one is the alteration of feldspars which explained by the abundant presence of potassium, barium and strontium in the opal and the second source of silica is alteration of volcanic glass. Indeed, the percolation of meteoric waters in ashes of ignimbrites can dissolve and mobilize the silica and from a concentrated solution of silica. This solution fills voids or is trapped in unwelded ignimbrite layers (Rondeau et al., 2012).

The crystallography of opal has controlled, at least in part, the incorporation of chemical impurities may form not well-crystallized opal. That is, although the Wegel Tena opals are poorly crystallized, they consist mostly of tridimensional networks of Si-O bonds (Chamard-Bois, 2015). The variation of opal is due to the silica-rich water did not circulate enough to homogenize the composition, nor to purify it from impurities (Rondeau et al., 2012). However, its properties are consistent with those of opal-CT and most volcanic opals. Inclusions consist of pyrite, barium manganese oxides, and native carbon. Some samples show “digit patterns”: interpenetrating play of-color and common opal, resembling fingers (Rondeau et al., 2010). The opaque-to-

translucent Wegel Tena opals become transparent when soaked in water, showing a remarkable hydrophane character (Chamard-Bois, 2015).

Wegel Tena opal has been suggested to be of pedogenetic origin, hence related to continental weathering (Rondeau et al., 2012; Chauvire et al., 2019). The weathered layer of the host rock shows a granular microstructure with coatings of illuvial clays in the pores (Chauvire et al., 2019). Opal acts as a cement for these typical pedogenic features, suggesting opal precipitation concomitant with or posterior to pedogenesis (Rondeau et al., 2012). Opal also fills the remaining porosity or large, up to decimetric, cavities. Therefore, opal formation is closely related to pedogenesis (Rondeau et al., 2012; Chauvire et al., 2019).

2.2.3 Stability

Gem opals from Ethiopia are often prone to cracking only with the course of time or just mild heating. This unfortunate effect is associated with appreciable water content in the open pores of the material. Internal stresses arise upon any dehydration resulting in surface shrinkage and progressive cracking and whitening (Filin and Puzynin, 2009).

Cracking and whitening are observed in Wegel Tena opal. Some samples crack even before cutting and polishing, and some others suffer from whitening (Filin and Puzynin, 2009; Rondeau et al., 2011). But, Wegel Tena translucent opal is more stable than transparent opal without considering their hydrophane character (Rondeau et al., 2010).

Evacuating water from non-hydrophane samples promotes cracking. Also, cracked samples can crack at heating, or show the propagation of new cracks. Hence in non-hydrophane samples water being linked to the silicate framework and the water detached from the internal structure when the sample is heated and the water is being released it creates enough internal stress and then leads to the development of new cracks. Cracks then propagate from an irregular surface or a pre-existing crack network. While the hydrophane opals do not crack because the lost water is molecular not being linked to the silicate framework (Dagnachew, 2017).

2.3 THE COLOUR SOURCE OF OPAL

The play-of-color is due to the diffraction of visible light on a perfect network of silica spheres having an adequate diameter, between 150 and 300 nm described by Sanders (1964). Common opals can still be very valuable as gems for their transparency and their body color which spans a large spectrum (Gaillou et al., 2008).

Klein et al. (1993) conducted that, interference of light either at the surface or in the interior of a mineral may produce a series of colors as the angle of the incident light changes. The striking flashes of varied color against a white or black background, as seen in precious opal, are called play of colors. Electron microscopic study of opal has revealed that the underlying reason for the color play is the presence (in precious opal) of a regular three-dimensional array of equal–size spheres (Fig. 2.1). These spheres consist of amorphous silica SiO_2, with small amounts of water; and they are cemented together. In precious opal, the uniformly packed spheres occur in patches (domains) ranging from less than a millimetre to more than a centimetre across.

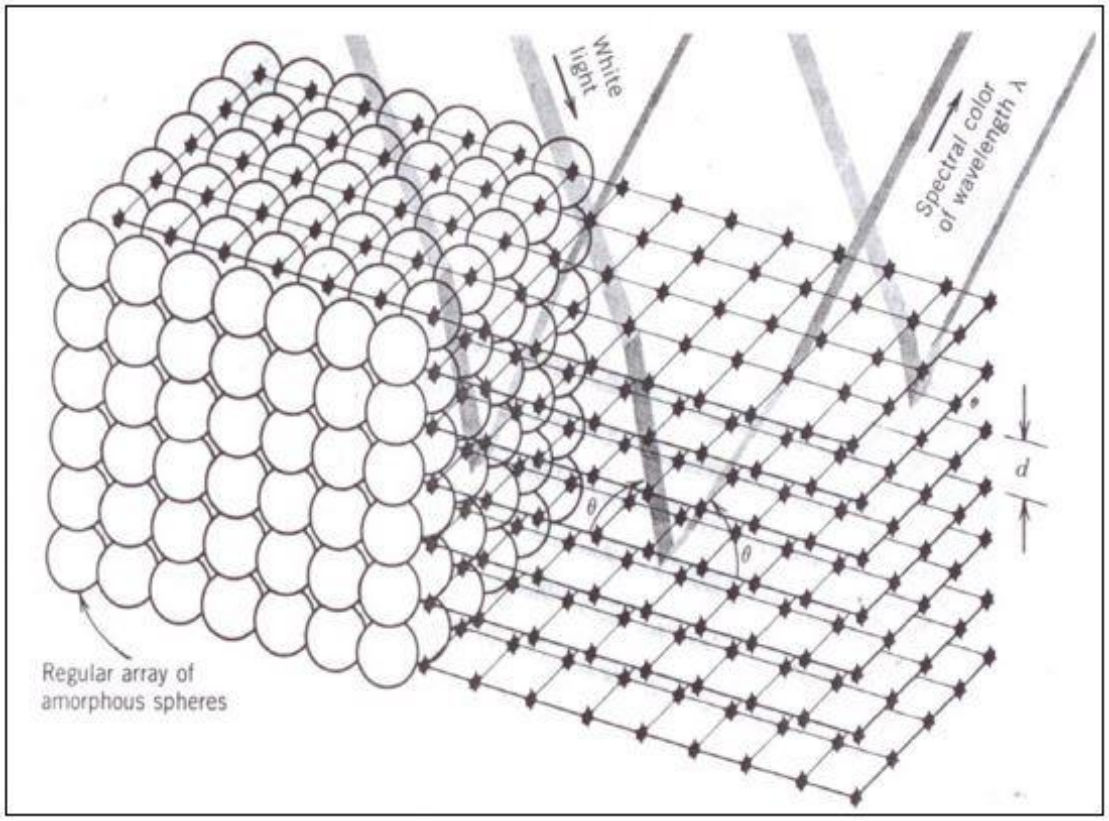

Figure 2.1: The spectral colors of precious opal are the result of diffraction by regularly spaced lattice planes. These planes result from amorphous spheres in a regular close-packed array (Klein et al., 1993).

According to Gaillou et al. (2008), the composition of opals influences some physical properties. Not surprisingly, color is often dependent on chemical impurities: almost all color opals are colored by impurities, while some are colored by mineral inclusions. Concentrations that are greater than 500 ppm are Al, Ca, Fe, K, Na, and Mg are the main impurities of opal. Other impurities may be present Such as Ba, Zr, Sr, Rb, U, Y, Pb, Mn, Zn, and Cu. Some of these elements may have an impact on the physical properties of opals. Even in low concentrations, for example, uranium luminescence of green color, the presence of iron in fire opals is responsible for the intensity of the color orange. The whole of these impurities may or may not be present in the opals and varying amounts. They are very often representative of the chemical composition of the host rock (Fritsch et al., 1999; Gaillou et al., 2008). In general, the body color in the opal mass is due to the presence of colored mineral inclusions (Chamard-Bois, 2015; Gaillou et al., 2008).

2.4 VALUE OF OPAL

On a scale of one to ten opal is easily the hardest gemstone to try and value. Opal has an infinite number of variables including color, pattern, brightness, and origin. Opal has a complicated classification system for valuations that is much harder than any other gemstone [(2a)].

Over many years there have been guidelines developed on how to value Opal. 10 factors that contribute to valuing an opal are:

1. **Color:** Color is the first thing that you will notice about an opal. In order of value, the most valuable color is black, red, orange, green, blue, and purple. The density and intensity of the color are also important to determine the price. The thickness of the color bar can help to amplify the brilliance of the opal color. Seam opal generally has a thinner color bar than opals formed in a knobby.
2. **Direction/Play of Color:** Opals are a gemstone that dramatically changes appearance based on what angle the opal is viewed at. When an opal is at its brightest, this is called ‘facing’. The direction of color can affect the price because it will determine how versatile the opal is.
3. **Pattern:** Opals that have a rare or unique pattern are more valuable. The Harlequin pattern is the rarest and most loved pattern in opals but it is very

rare. Some top patterns are mackerel, block, broad flash, rolling flash, pin fire. Opals that have no or only slight patterns are generally less valuable.

4. **Body tone:** body tone is one of the most important factors in the classification and valuation of opals. Body tone refers to the background or the underlying color of the opal, which ranges from black through the dark to light. Generally, opals with a black or dark body tone are more valuable than those with a white, light, or crystal body tone.
5. **Brightness:** The opal brightness guide was produced by the Australian opal association along with the body tone guide. The brighter the opal, the more expensive will be its value.
6. **Shape:** Oval stones are generally considered more valuable than free form, except with boulder opals where the free form is considered desirable. The shape of the opal once again determines how versatile it is. Oval stones generally have the best face of color and can be used in a variety of applications. Opal is almost always cut in a cabochon. A cabochon stone is more valuable when it has a high dome compared to a flat stone.
7. **Inclusions:** Inclusions and potch lines are not to be confused with cracks. A crack line reflects light and greatly devalues an opal. A potch line has no light reflection and these opals are generally valued lower but can make artistic picture patterns.
8. **Which Opal Field:** The end buyer or wholesaler might not be able to consider this factor. But in the trade certain mines have a reputation of producing good quality rough that makes excellent stones. Even the depth of the mine can greatly affect value.
9. **Natural vs. Treated:** Natural opal is always valued higher compared to treat opal.
10. **Country Origin:** Australia has a worldwide reputation as the world's most expensive opal. Many countries now produce good opals like Ethiopia, Mexico, and Brazil. Each country's opal may be unique and this factor helps to determine the opal price.

2a (https://www.opalauctions.com/learn/how-tos/how-to-value-opal)

2.4 SOME KNOWN WORLD OPAL MINERAL

Opal occurrence is distributed along with different parts of the world (Fig. 2.2). Australia produces the world's largest variety of opals and controls the world market (Dowell et al., 2003; Dutkiewicz et al., 2013). Opals can also be produced from Ethiopia, Mexico, Brazil, and USA which all have their color and pattern attributes (Gaillou et al., 2008). No other stone can match opals. The uniqueness of owning a stone that no one else owns is the advantage of opals.

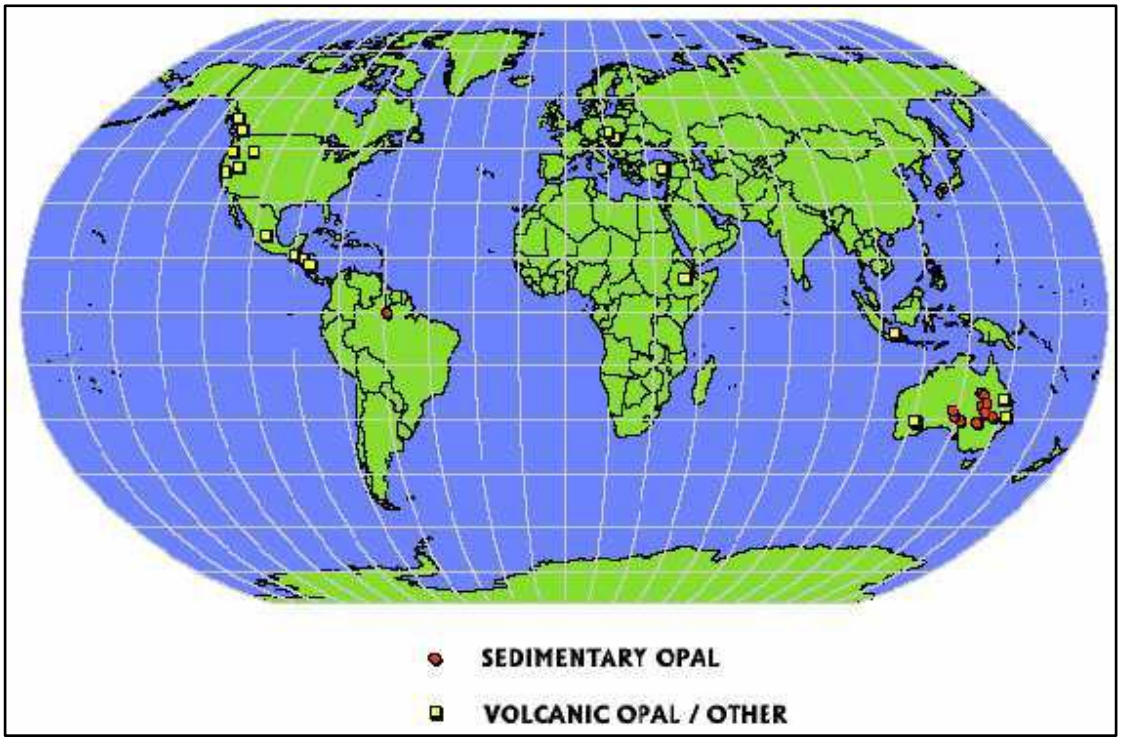

Figure 2.2**:** Precious opal deposits of the world (Horton, 2002).

2.4.1 Australian opal

According to Croll (1950), the first precisely recorded discovery of precious opal was at two localities in Queensland at Listowel Downs, north-east of Adavale, and at Springsurein 1872. The next important discovery was in 1915 when opal was found at Stuarts Range in northern South Australia. The field developed from this discovery was called Coober Pedy. It is a major source of opal including the largest and most valuable opal, the Olympic Australis. Thus Australia makes opal the country's national gemstone.

Opal is predominantly found in Australia, virtually most opal deposit is sedimentary opal-A with supplying over 95% of the world's precious opal (Dutkiewicz et al.,

2013). The opal occurs almost exclusively within Cretaceous sedimentary rocks (Dowell et al., 2003; Dutkiewicz et al., 2013). All of the significant opal deposits in Australia occur in the Great Artesian Basin. Additionally, milky-white opals are common in Coober Pedy, White Cliffs, and Andamooka; boulder opals are mined in Southern Queensland and black opals are mined at Lightning Ridge (Dowell et al., 2003).

Dutkiewicz et al. (2013) conducted that, intense weathering resulted in extensive silicification, and then weathering of feldspars provided ample silica-rich fluids for the formation of opal. The opal frequently occurs as cm to dm-thick bands or pockets at the interface between shale and sandstone filling primary and secondary pore spaces and fractures and is usually found down to 30 m below the surface (Dutkiewicz et al., 2015).

2.4.2 Mexican opal

Mexico is the second-largest producer of opal (Gaillou et al., 2008). The opals are known for their vivid yellow, orange or orange-red colors. The intense color has earned this gem the nickname fire opal. But it makes up for this with its remarkable body-color [(2b)].

Mexican opal is considered a mineraloid and has no crystal structure. The term used for no structure is amorphous. It displays a play of color but is rare because volcanic opal forms relatively quickly and the spheres of silica rarely have time to settle into the diffraction grids that create play of color [(2c)].

Mexican opal has been known since the latter part of the 18th century, but the more familiar gem-quality material has been available to the world market only since the end of the last century. The most important opal deposits in Mexico are in the state of Queretaro, although there are other significant deposits in the states of Chihuahua, San Luis Potosi, Guerrero, Hidalgo, Jalisco, and Michoacan (Koivula et al., 1983; Coenraads and Zenil, 2006). However, Queretaro is the centre of opal mining and cutting in Mexico, and it is the predominantly reddish-orange fire opal (Koivula et al ., 1983).

2b (https://www.google.com/search?q=mexico+opal&ie=utf-8)

2c (https://www.ajsgem.com/gemstone-information/mexican-opal-96.html)

Based on the study of Koivula et al. (1983), the opal occurs in a series of thinly bedded rhyolite lava flows. Locally these pink to brick-red rhyolites exhibit an abundance of irregular to oval lithophysal (gas) cavities common to rhyolitic lava flows. The opal occurs as a secondary filling in these cavities as well as in any other available spaces in the lava, including pumice fragments and fractures. The opal usually fills the cavities, but occasionally it is found as loose nodules in the open spaces. These loose nodules, which may be "as large as a hen's egg," are generally the highest quality material.

2.4.3 Brazilian opal

Brazil is also the largest producer of opal for the world market. The strip of land exploited for the production of opal is located in the region that is made up essentially of sub-horizontal sandstones of the Cebecas formation of the Palaeozoic era, intercalated and/or cut with sills and dikes of diabase and Triassic basalt (Barreto and Bittar, 2010).

According to Barreto and Bittar (2010) opal occur in three different ways:

- ✓ In alluvium and colluvium resulting from the breaking up of the rock source opals
- ✓ in veins, filling fractures in the diabase and in the sandstone, principally areas where these two kinds of rock come in to contact and
- ✓ Near the upper contact zone of diabase sills with sandstone.

Brazilian opal has tended to be white semi-transparent through to a see-through body tone. Though a Boi Morto vein obtained a small amount of black opal a few decades ago. The largest opal found in Brazil weighed an astonishing 4.3 kg. Brazilian opal is mined in the northeast region of the state of Piaua, where there are no large-scale opal fields and the only equipment used is a generator. Many Brazilian opals are found in a quarry at the foot of a sandstone cliff and are hand-dug [(2d)].

Brazilian Opal has a lower possibility to crack due to exposure to heat or sunlight. It has also been noted that Brazilian opal is somewhat tougher compared with other Opals[(2d)].

2d (https://www.opalauctions.com/learn/a-z-of-opals/brazilian-opal-information)

CHAPTER THREE

3. REGIONAL GEOLOGY

3.1 INTRODUCTION

The geological evolution of Ethiopia, with alternating phases of orogenesis, peneplanation, crustal updoming, faulting, emplacement of huge amounts of lava, and deep fluvial dissection has imprinted the geomorphological landscapes of the country with specific characteristics, in places unique on Earth (Abbate et al., 2015). The country is characterized by different types of rocks. It is covered by 18% Precambrian basement rock, 25% Mesozoic sedimentary rock, and 56% Cenozoic volcanic and sediments (Gerra, 2000).

3.2 ETHIOPIAN PLATEAU VOLCANIC PROVINCE

The Ethiopian plateau is one of the intraplate volcanism in northeastern Africa (Wilson and Guiraud, 1992) and forms the largest part of extensive continental flood basalt province which resulted from mantel plume-head activity (Davies et al., 2003; Wilson and Guiraud, 1992). It is dominated by a Tertiary and Quaternary basaltic pile, fed from fissures aligned along developing pairs of opposed, nascent continental margins (Mohr, 1983). The Cenozoic Ethiopian continental flood basalt province is located at the junction of three rifts: two oceanic rifts, the Red Sea and the Gulf of Aden, and the East African continental rift. The main part of the province crops out in Ethiopia, whereas the rest is located on the eastern side of the Red Sea, in Yemen (Pik et al., 1998). In Ethiopia, this huge volume of lavas about 350,000 km^3 which forms a pile up to 2,000 m thick, and covers more than 600,000 km^2 (Berhe et al., 1987; Mohr, 1983; Mohr and Zanettin, 1988) was erupted 30 Ma ago, before the significant extension (Pik et al., 1998).

Berhe et al. (1987) conducted that, volcanism in Ethiopia began as early as the Eocene in two restricted areas of Flood Basalts: (i) NW/Central Ethiopia (<40 Ma) and (ii) SW Ethiopia (49 Ma). The main volcanic successions were developed over a broad region during the Oligocene-Miocene in Ethiopia.

The Cenozoic volcanic rock of Ethiopia is divided into Trap and Aden series. Trap series is used to refer to the whole pile of the tertiary flood basalt sequence with

intercalations of felsic lava and pyroclastic rock which forms a southwestern and southeastern plateau. The term Aden series used for post-rift (middle Miocene to Quaternary) volcanic rock of the main Ethiopian rift, Afar Depression, and some part of the Ethiopian plateau (Mohr, 1962).

3.2.1 Northwestern Ethiopian plateau

In northwest Ethiopia, the early Cenozoic extension and/or faulting is accompanied by widespread volcanism (Berhe et al., 1987; Pik et al., 1998).

The northern Ethiopian plateau mainly consists of tholeiitic to transitional basaltic lavas (Mohr and Zanettin, 1988), which were erupted at ~30Ma in a period of 1Myr or less (Hofmann et al., 1997). The basalts cover an area of ~210 000 km^2 with a lava pile up to 2000m thick in the central-eastern part, thinning to less than 500m toward the northern and southern boundaries. On the eastern margin, neighbouring the Afar escarpment, rhyolitic volcanic rocks characterizing the upper part of the sequence have been interpreted as the differentiated products of basaltic magmas that mark the start of continental rifting (Ayalew et al., 2006).

Pik et al. (1998, 1999) have classified the north-western Ethiopian flood basalts into three distinct geochemical groups based on trace element and Ti concentrations: low-Ti basalts (LT), high-Ti1 (HT1) basalts, and high-Ti2 (HT2) basalts (Fig. 3.1). They recognized a suite of 'low-Ti' (LT) basalts restricted to the northwestern part of the province, are quantitatively predominant (150,000 Km^3) (Baccaluva et al., 2009), and assumed to be derived from the depleted mantle. They are characterized by relatively flat REE patterns and lower Ti and incompatible trace element concentrations. Alkali basalts found to the south and east of the province on the other hand show higher concentrations of incompatible elements and more fractionated REE patterns and related to the so-called 'high-Ti' basalts (HT1 and HT2).

The LT basalts display the lowest TiO_2 contents (1–2.6%) and relatively high SiO_2 (47- 51%) (Pik et al., 1998; Baccaluva et al., 2009). It corresponds to the low-Ti magma type, commonly described in CFB provinces. The LT basalts display a strong lithospheric signature characterized by relative depletion in Nb, Ta, Th, and Rb compared to oceanic basalts. The geochemical compositions observed in this basaltic group are strongly variable and lead to a wide range of values for incompatible trace

element ratios such as La/Nb, Ce/Pb, Ba/Th, and Ba/La (Pik et al., 1998, 1999). It mostly plots in the sub alkaline field, showing the widest differentiation range (Baccaluva et al., 2009).

In contrast, the two (HT1 & HT2) groups display much higher TiO_2 contents. The HT2 basalts display opposite geochemical characteristics with low SiO_2 (44-48.3%): the observed compositions are much more homogeneous and fall in the OIB compositional range. The HT1 basalts display compositions intermediate between those of LT and HT2 basalts, also have a typical high-Ti signature (Pik et al., 1998, 1999).

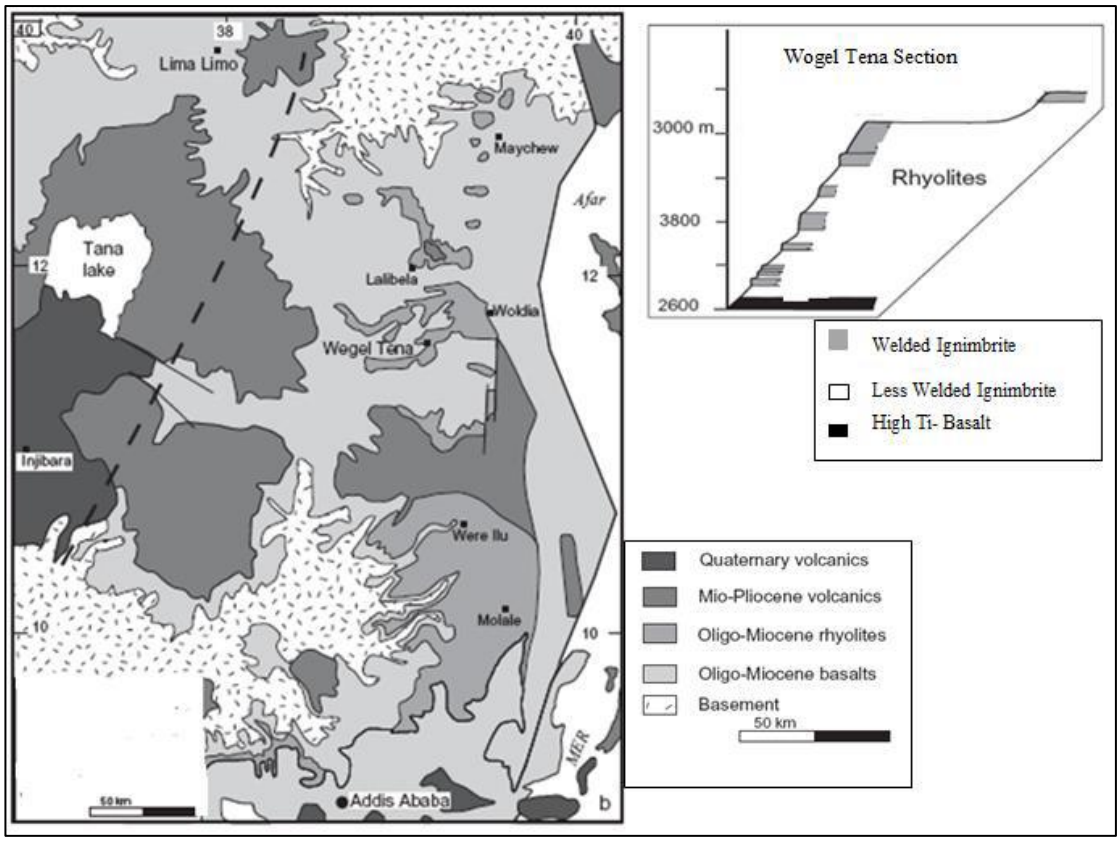

Figure 3.1: Location map of northern Ethiopian Plateau volcanic province, Afar Rift, and Main Ethiopian Rift (after Merla et al., 1979). The approximate broken line separates the low-Ti and High-Ti flood basalt province of Pik et al. (1998) with stratigraphic profiles of Wegel Tena sections after the work of Ayalew and Yirgu (2003).

According to Demissie et al. (2010), the area comprises four major groups of the Cenozoic volcanic rocks i.e Eocene-Oligocene, ii. Oligocene-Miocene, iii. Late Miocene and Quaternary volcanic rocks and associated lacustrine and superficial sediments.

Eocene-Oligocene comprises the Ashangie basalts and Wegel Tena rhyolitic ignimbrite. Dessie basalt Formation and Tarmaber-Megezez Formation are part of Oligocene-Miocene. Late Miocene comprises Kemise rhyolite and Dalha Formation. Adami basalt, Wederage basalt, Merto rhyolite and undifferentaited alluvial, elluvial and lacustrine sediments included in Quaternary volcanic rocks and associated lacustrine and superficial sediments.

CHAPTER FOUR

4. GEOLOGY OF THE STUDY AREA

4.1 GENERAL OVERVIEW

The study area is mostly covered by basaltic lava flow and pyroclastic deposits of Cenozoic volcanic rock (rhyolitic ignimbrite) (Fig. 4.1). The lithological units exposed in the study area are characterized by a range of composition. The rock units are identified and described based on their color, mineral composition, texture, in-hand specimen, and exposure level. Accordingly, three main mappable units are identified. These are vesicular basalt, rhyolitic ignimbrite, and lower basalt. Out of the three identified units, rhyolitic ignimbrite and lower basalt are the dominant ones, covers a wider area, whereas, vesicular basalt is less outcropped and covers a smaller area (Fig. 4.6). Rhyolitic ignimbrite is the primary focus of this study since opals are hosted by it. Gentle slope, highly weathered, and undulating topographic lower basalts cover the lower most of the volcanic sequence. The rhyolitic ignimbrites overlie directly on the lower basalt in the eastern and southern parts. Lower basalt is also overlain by vesicular basalt in the northwestern part of the study area.

Generally, three active mining sites were visited. Gem opal occurs in one horizon within an unwelded rhyolitic ignimbrite bed. These mines are all located on the steep sides of the plateau, where the opal-bearing horizons outcrop (Fig. 4.3). The opal-bearing horizon is concordant with the layering and the elevation is between 2700 and 2800 m. The layer is strongly weathered, altered volcanic glass, granular microstructures cemented by opal, and cavities are filled by clay. Rock units exposed in the study area are described in the subsequent sections.

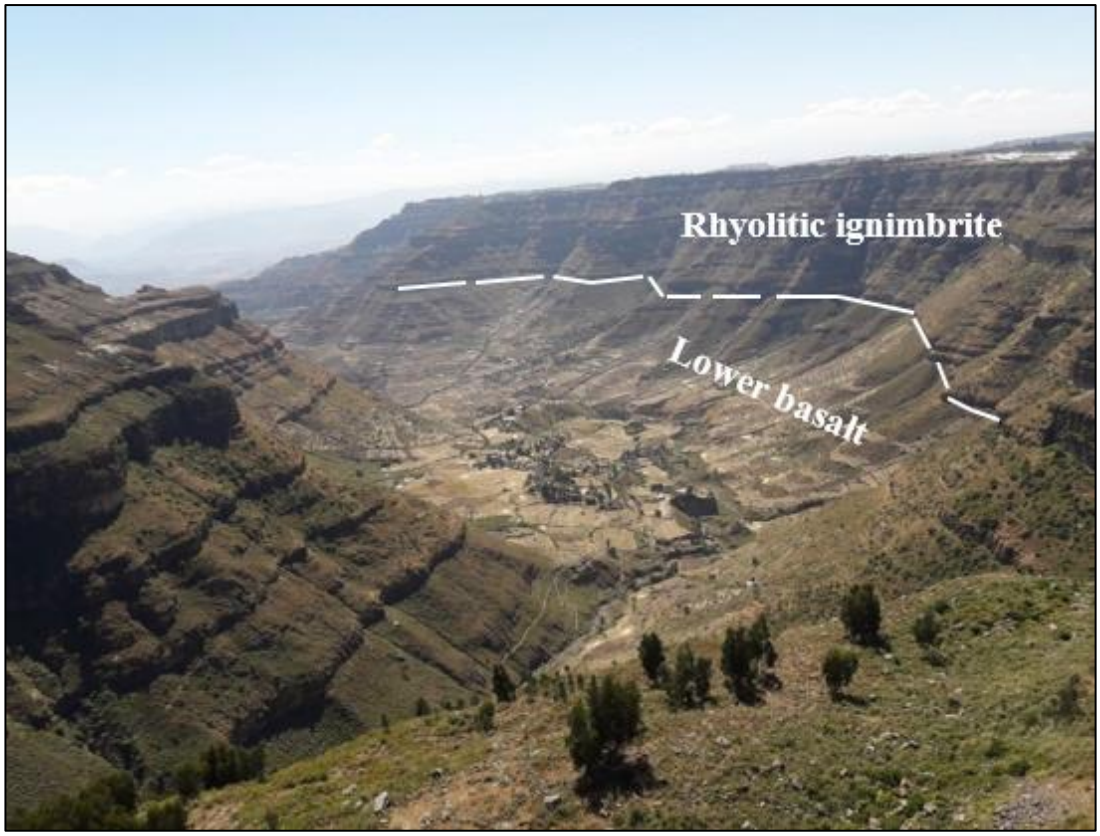

Figure 4. 1: A typical viewpoint onto Worke Washa locality to the eastern part of the study area, showing different lithologies and layers of the volcanic sequence.

4.2 LOWER BASALT

Black to dark grey, and greenish-grey in color, aphantic to porphyritic in texture (Fig. 4.2) with varying thickness. These basalt flows represent the lower most parts of volcanic successions (Fig. 4.1). The rock unit is exposed dominantly in the southeastern, eastern, and southern tip of the study area. It also exposed along the deep river gorges in some parts of the area, road cuts, stream beds, gentle and steep slopes of undulating mountain chains, and low-lying flat plains. The unit is overlain by the rhyolitic ignimbrite at the southern and eastern parts of the study area.

Figure 4. 2: Lower basalt.

4.3 RHYOLITIC IGNIMBRITE

The rock is pink, white, brown and light to dark grey, coarse-grained and has a thickness varying from 400 to 700 m. It is exposed in most of the central, southwestern, southern, and northeastern parts of the study area (Fig. 4.6). It is highly eroded, cliff-forming, and dissected by the deep gorges. The unit is layered and individual layers vary in thickness from 2.5 up to 15 m (Fig 4.3). The layers show variation in texture, thickness, and intensity of weathering conditions. The rock unit is the host rock for opal minerals and at the middle a very thin layer, not more than 3m thick lithostratigraphic position of opal bearing zone (Fig. 4.3).

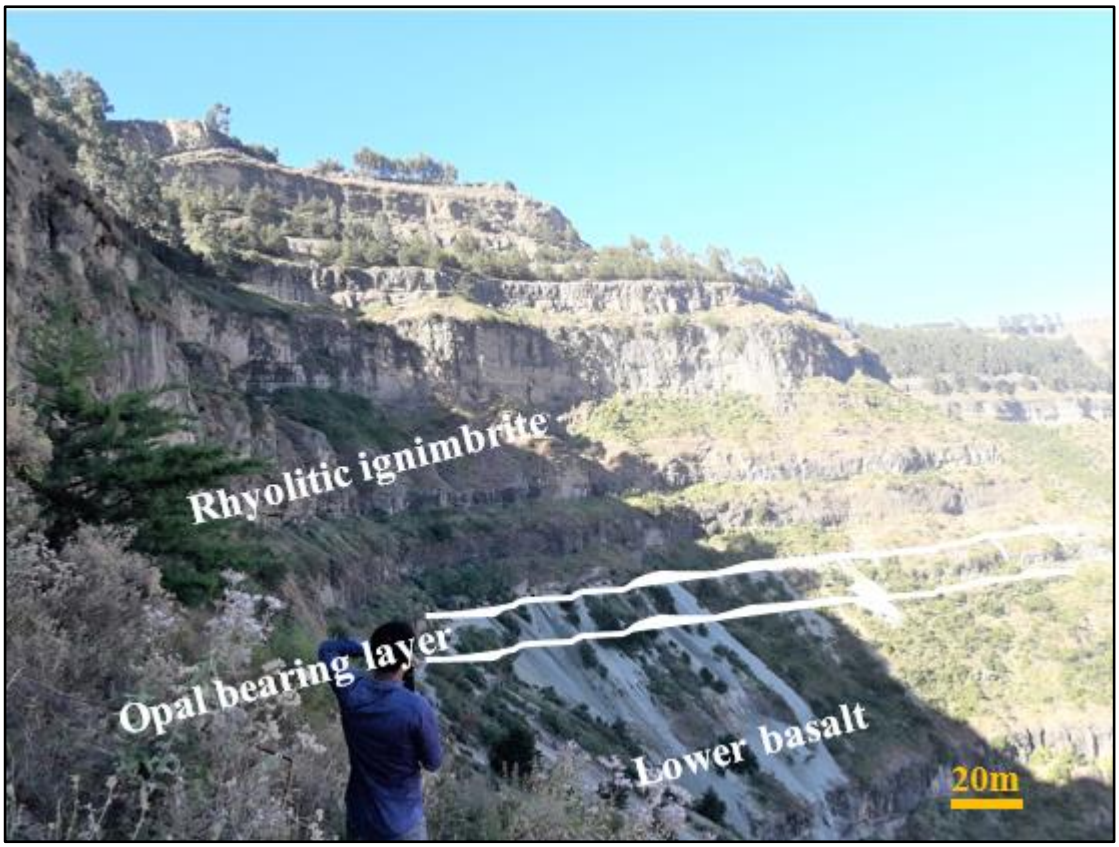

Figure 4. 3: General lithostratigraphy of the study area (photo from Worke Washa locality) showing the lower basalt below the opal bearing layer, and the upper parts of the rhyolitic ignimbrite forms steep cliff with an alternating layer of both welded and unwelded, and at the middle a very thin layer, not more than 3m thick of opal bearing horizon.

Based on the field investigation, there are three different types of layers observed in this rock unit. These are: I) highly welded, and unweathered (Fig. 4.4A),

II) less welded, and moderately weathered (Fig.4.4B) and

III) unwelded, and highly weathered layer (Fig. 4.4C).

Higly welded ignimbrites have a glassy appearance and exhibit a well-developed columnar jointing structure mostly on the upper parts of the succession and forms steep cliff with an alternation with less welded layer . Unwelded and highly weathered layer hosts gem opal on the area. This opal bearing layer is brownish, soft, and friable, affected by intense weathering and clay-rich horizon (Fig. 4.4C).

Figure 4. 4: A) highly welded, and unweathered B) unwelded, less weathered, and non-opal bearing and C) unwelded, affected by intense weathering and opal bearing layer of rhyolitic ignimbrite.

4.4 VESICULAR BASALT

This lithological unit has black to dark grey, vesicular with minor aphantic to sub porphyritic texture (Fig. 4.5). It is exposed by forming a chain of ridges, cliffs along the escarpment of Zita river cuts, and tributary streams of the Zita River. This Vesicular basalt is exposed dominantly to the northwestern part and underlain by rhyolitic ignimbrite(Fig. 4.6).

Figure 4. 5: Vesicular basalt.

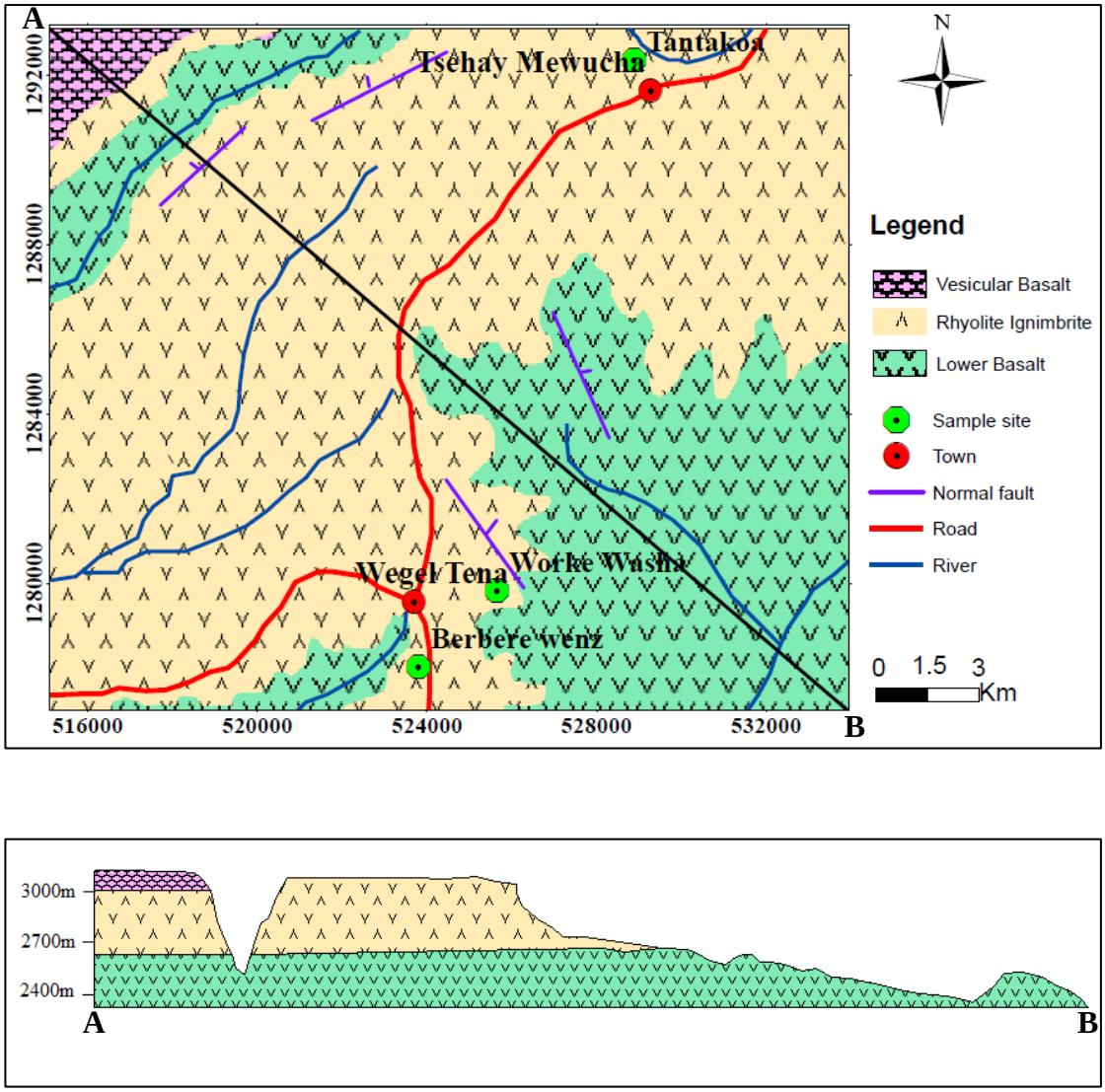

Figure 4. 6: Geological map of the study area adopted after Demissie et al., (2010) and cross section for line A-B.

4.5 PETROGRAPHIC RESULTS OF THE HOST ROCK

Representative rock samples have been collected in the field and examined for their mineral assemblages and textural characteristics using a petrographic microscope. The samples collected for the petrographic study are from three different sites (Tantakoa, Worke Washa, and Berbere Wenz) where local artisanal mining activities are held (Fig. 4.7). During sampling, the samples were taken from the mining tunnel (50-100 m) horizontally to obtain the representative samples.

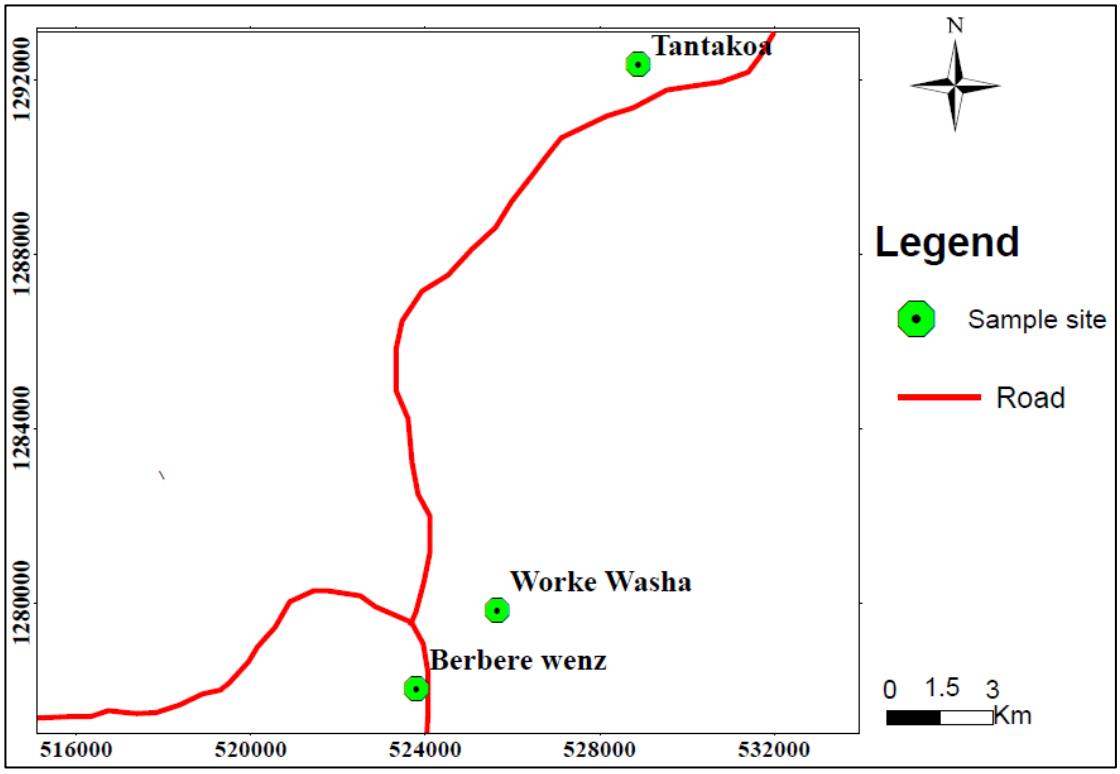

Figure 4.7: location map of sample sites.

The petrographic examination result shows similar petrography at all investigated sites. They are composed of quartz, plagioclase, sanidine, biotite, hornblende, lithic-fragment, and opaque (Fe-oxide) form the framework of this rock mass. The matrix is composed of fine-grained groundmass (>75%), occasionally welded and mostly weathered. Some slight variations in the opal-bearing horizon from one mine to another. At Berbere Wenz, opal cements a highly weathered rock, and clay material is apparent, whereas, at Tantakoa, and Worke Washa sites, the host rock is characterized by less amount of clayey material than Berbere Wenz. Description of thin sections and photomicrographs of representative rock samples are discussed subsequent sections.

The modal proportion of each rock sample was visually estimated using a petrographic microscope. A simple estimation technique was used for modal average composition. The mineral modal proportion of all rock samples are summarized in annex-B.

4.5.1 Samples from tantakoa area

Four host rock samples (TAT-100A, TAT-100B, TAT-100C, and TAT-101B) were examined for their petrographic characteristics. Similar petrographic properties were observed in the four samples. The samples are composed of brown to light grey, fine-grained groundmass (75-85%), and different size phenocrysts (20-25%) which are surrounded by a fine-grained matrix (Fig. 4.8). The phenocrysts include anhedral, randomly distributed quartz; elongated, anhedral to subhedral plagioclase; anhedral, characterized by simple twining, randomly distributed sanidine; pleochoroic, anhedral to subhedral biotite; fine-grained, irregular, randomly distributed xenoblastic opaque minerals and lithic fragments. The rock (lithic) fragments are of rhyolite and pumice.

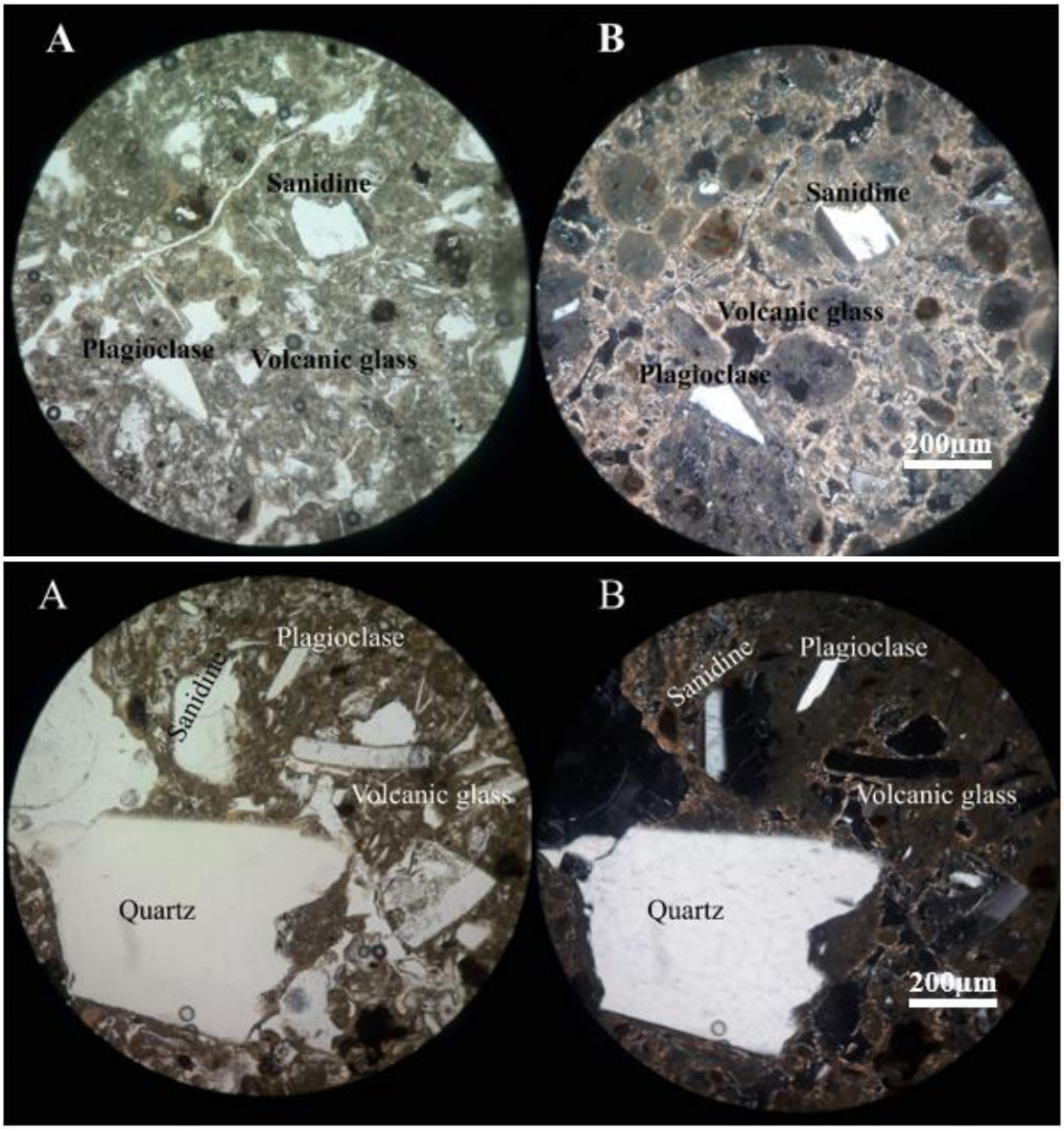

Figure 4.8: Microphotograph of sample TAT-100A, and TAT-101B showing various mineralogical and textural features taken under 10x magnification power respectively. **(A)** PPL and (B) XPL showing crystals of plagioclase, quartz, and sanidine; the crystals are anhedral and embedded by fine-grained groundmass.

4.5.2 Samples from worke washa area

KOW-200A, KOW-200B, KOW-200C, and KOW-200D were the samples examined for their mineralogical assemblage and textural characteristics. It is composed of brown to light grey, fine-grained groundmass >80% for all samples, and phenocrysts <20%, and nearly similar petrographic properties in the five samples. Anhedral quart; elongated, anhedral to subhedral plagioclase; sanidine characterized by simple twinning; bluish to yellow biotite; light green to brown hornblende; randomly

distributed opaque minerals and lithic fragments of rhyolite and pumice forms the frame-work of the rocks (Fig. 4.9).

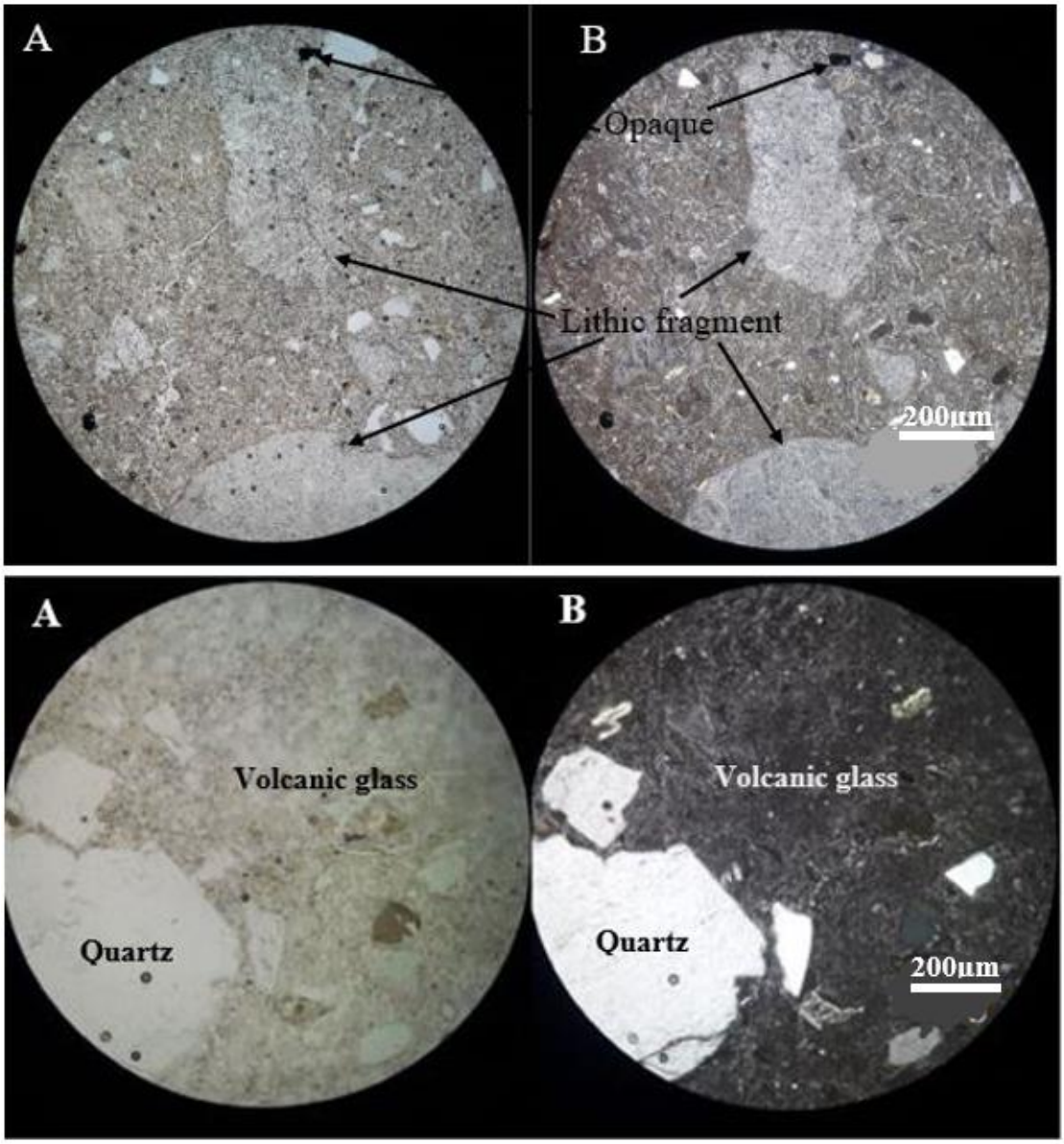

Figure 4. 9: Microphotograph of samples KOW-200C, and KOW-200D showing various mineralogical and textural features taken under 10x magnification power. **(A)** PPL and (B) XPL showing crystals of quartz and lithic fragments embedded by fine-grained groundmass.

4.5.3 Samples from berbere wenz

Five rock samples (BEW-300A, BEW-300B, BEW-300C, BEW-300D, and BEW-301A) were examined. The samples are composed of brown to light grey, fine-grained groundmass of volcanic glass (78-80%) for all samples, and phenocrysts (<20%) which are surrounded by a fine-grained matrix (Fig. 4.10). Quart, plagioclase,

sanidine, hornblende, opaque minerals, and lithic fragments form the framework of the rock.

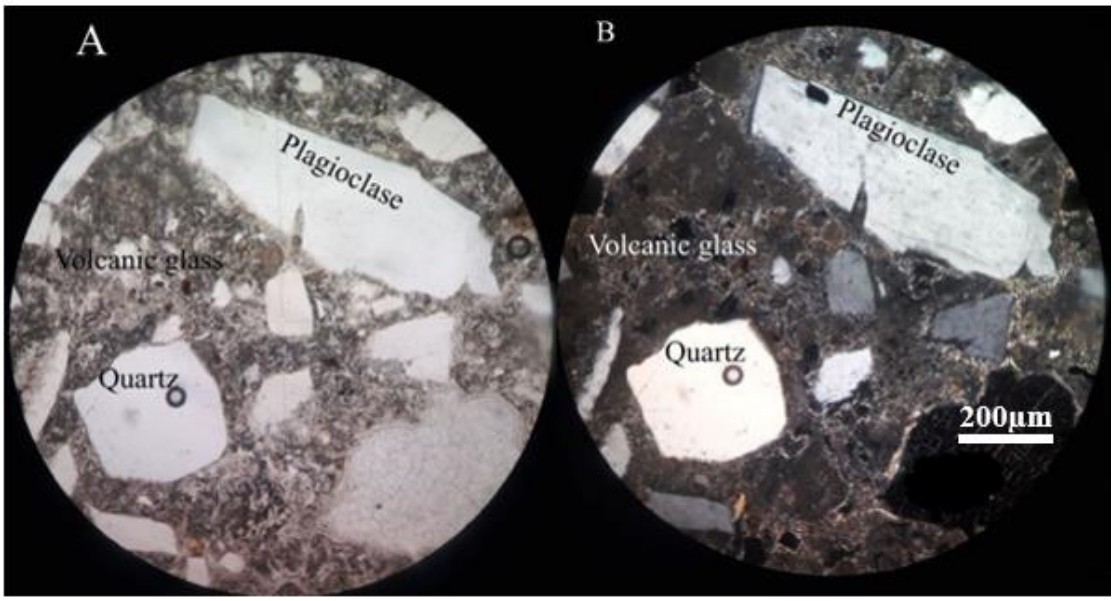

Figure 4. 10: Microphotograph of sample BEW-301A taken under 10x magnification power. **(A)** PPL and (B) XPL showing crystals of plagioclase and quartz embedded by fine-grained ground mass.

CHAPTER FIVE

5. GEOCHEMISTRY RESULTS

5.1 INTRODUCTION

The whole-rock composition of ten representative rock samples (Fig. 4.7) of the host rhyolitic ignimbrite was analyzed for major and trace elements. Additionally, three opal samples were analyzed for trace elements and the results are presented below. The geochemical study primarily targeted the host rock and opal minerals of the area to outline their relationship.

5.2 MAJOR ELEMENTS

Among the major elements SiO_2, Al_2O_3, and Fe_2O_3 show high values relative to other major oxides. The host rhyolitic ignimbrite has SiO_2 ranges between (56.2-64.6 wt.%), and Al_2O_3, Fe_2O_3, MgO, CaO, Na_2O, K_2O, and P_2O_5 13.25-14.50 wt.%, 4.90-8.01 wt.%, 0.63-1.21 wt.%, 1.10- 2.68 wt.%, 1.17-2.11 wt.%, 1.39-2.72 wt.%, and 0.01-0.52 wt.% respectivelly. These rocks have experienced various degrees of weathering indicated by the high value of loss on ignition (10.65 – 14.85 wt. %). The results of major elements of the host rock composition are presented in annex-C.

On Winchester and Floyd (1997) volcanic classification diagram (Nb/Y Vs $Zr/TiO_2x0.0001$) five samples (KOW-200B, KOW-200C, KOW-200D, BEW-300A, and BEW-300B) fall in the field of rhyolite, two samples (BEW-300C, and BEW-301A) in the field of trachyte-comendites/pantellerites boundary and three samples (TAT-100A, TAT-100C, and TAT-101B) sample in the field of trachy-andesite (Fig. 5.1).

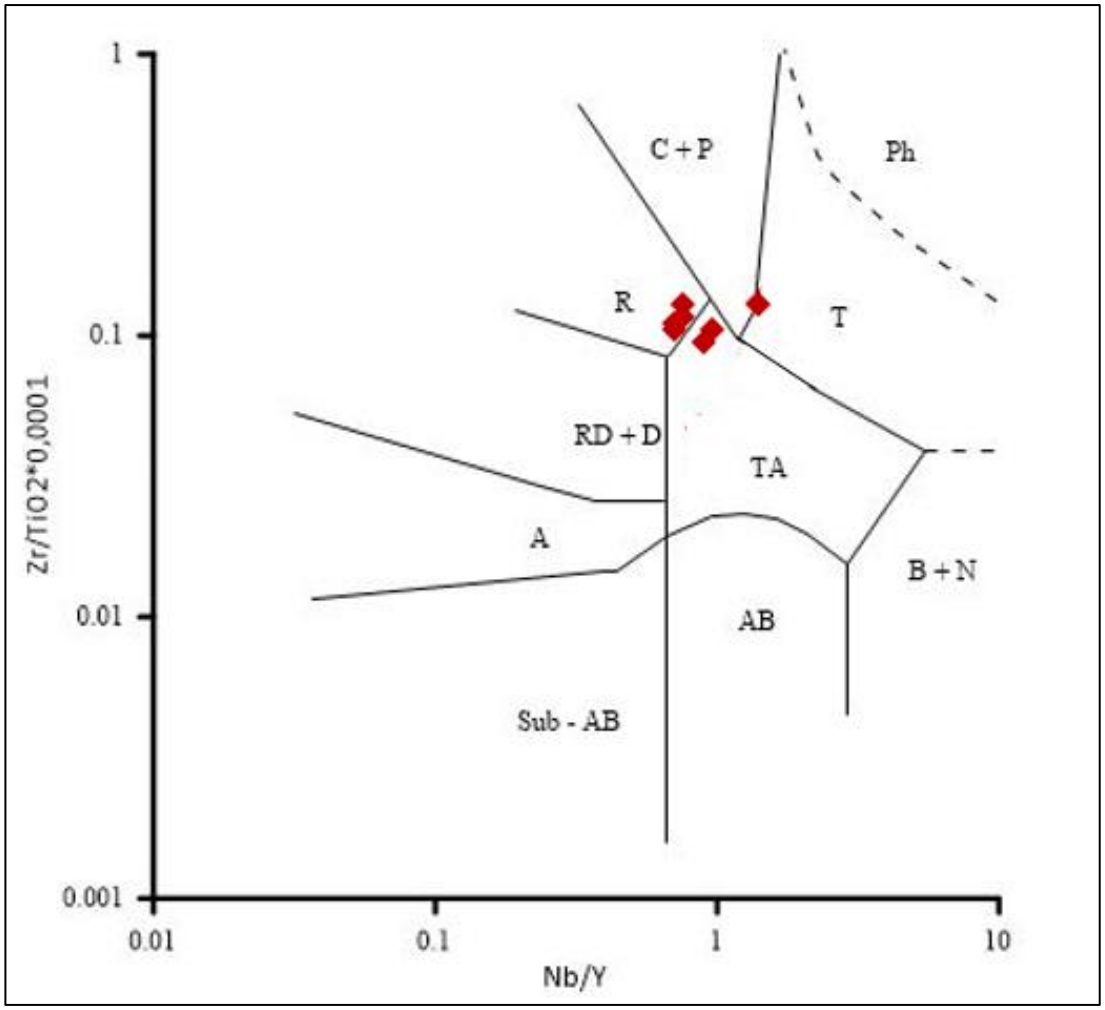

Figure 5.1: Nb/Y Vs $Zr/TiO_2x0.0001$ plot after Winchester and Floyd (1997) of the host rock. [Ph= phonolite, C+P= comendites/pantellerites, T= trachyte, R= rhyolite, TA= trachy-andesite, RD+D= rhyodacite/dacite, A= andesite, AB= alkali-basalt, B+N= basantine/nephelinites, sub-AB= sub-alkaline basalt].

Harker variation diagram is plotted, SiO_2 (wt. %) versus major oxides (wt. %) (Fig. 5.2). Major oxides like Fe_2O_3, CaO, MgO, TiO_2, and P2O5 decrease as SiO_2 increases and K_2O, and Na_2O shows a positive correlation with SiO_2. Generally, the plot shows near systematic variation of major oxides Vs SiO_2 when the elevation decreases from 2780 m (Tantakoa) to 2720 m (Berbere Wenz).

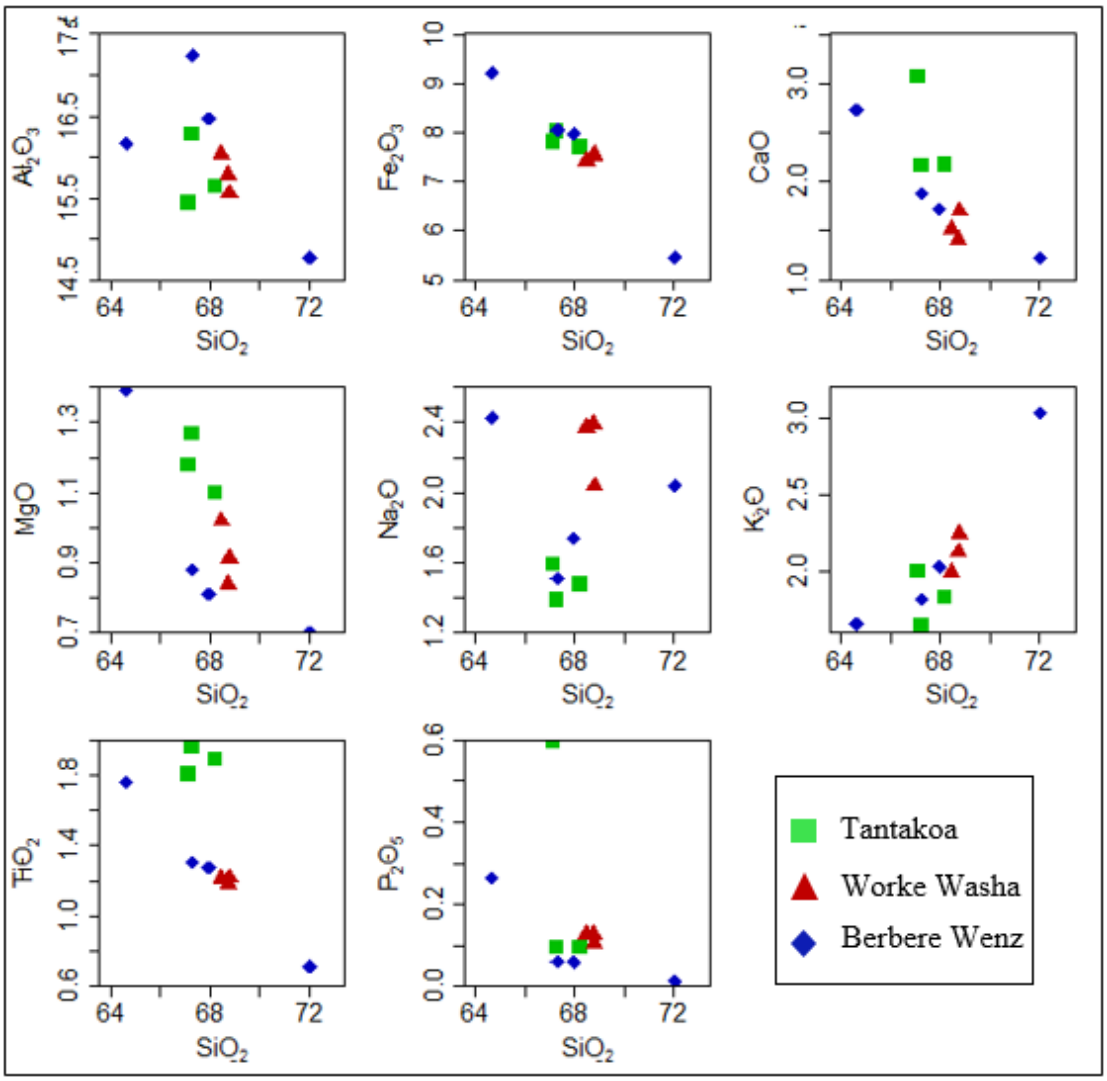

Figure 5.2: Harker variation diagrams SiO_2 (wt. %) versus major oxides (wt. %) of the rhyolitic ignimbrite of the study area.

5.3 TRACE ELEMENTS

Both trace elements and REE are detected from the analytical results of the host rock and opal samples. The rhyolitic ignimbrite is variably enriched in the whole range of trace elements, such as Zr (483.0-1540), Rb (46.8-95.0), Y (37.5-121.0), Nd (44.9-149.5), Nb (62.7-183.5), Ba (293-598), La (48.1-129.5), Sr (77.1-265), and Ce (111.5-313.0). Enriched trace elements in opal samples are, Zr (10.5-68.8), Ba (18.40-31.79), Nb (2.05-21.49), Ce (0.334-15.55), Sr (10.52-70.17), and Rb (2.81-17.28) ppm. The total result of the trace element composition of the host rock and opal samples are presented in annex-D in alphabetical order.

5.3.1 Trace element geochemistry of opal host rock

Multi-elements and REE patterns presented in this part are normalized to primitive mantle and chondrite (C1) respectively to compare directly the compositions of host rock and opals. Normalization values are from Sun and McDonough (1989).

The samples show nearly typical patterns for rhyolite in multi-element diagrams (Fig. 5.3). They show negative anomalies of Ba, K, Sr, P, and Ti which are possibly the consequence of fractionation of alkali feldspar (Ba and K), plagioclase feldspar (Sr), apatite (P), and Fe–Ti oxide (Ti). This observation suggests that the host rock were derived from basaltic parents through protracted crystal fractionation (Ayalew and Yirgu, 2003). They show an almost subparallel gentle REE pattern with a more or less pronounced enrichment in LREE compared to HREE. The analyzed rhyolitic ignimbrites are all light REE (LREE) enriched and have relatively unfractionated heavy REE (HREE) patterns (Fig. 5.4). In general, very weak (for sample BEW-301A) or absent Eu anomalies were observed in the host rock.

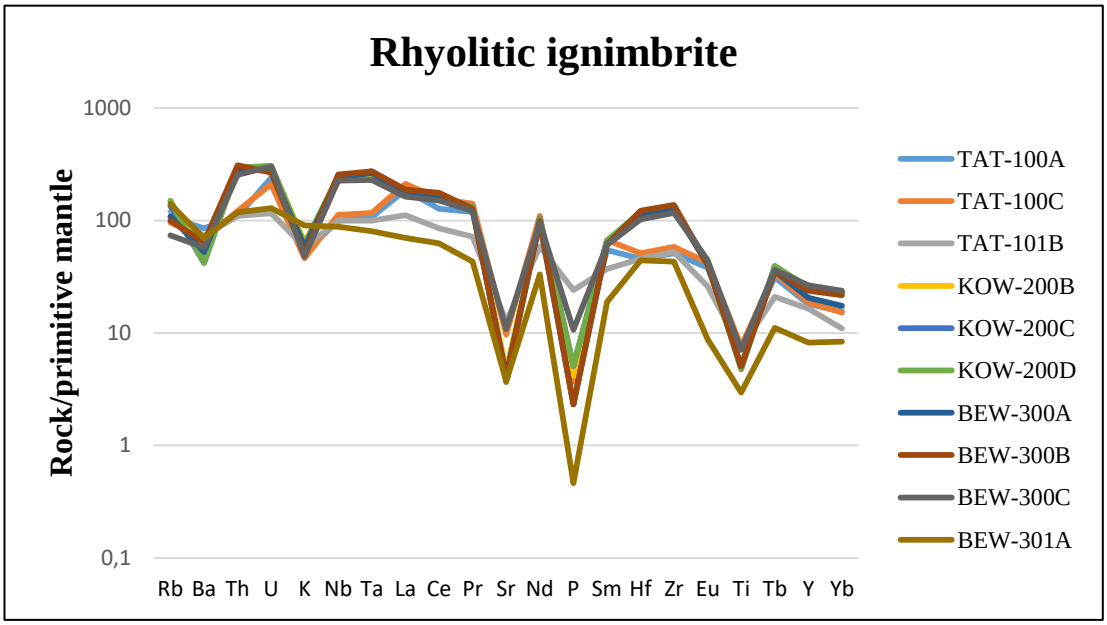

Figure 5.3: Multi-element diagram of Delanta opal's host rock normalized to primitive mantle.

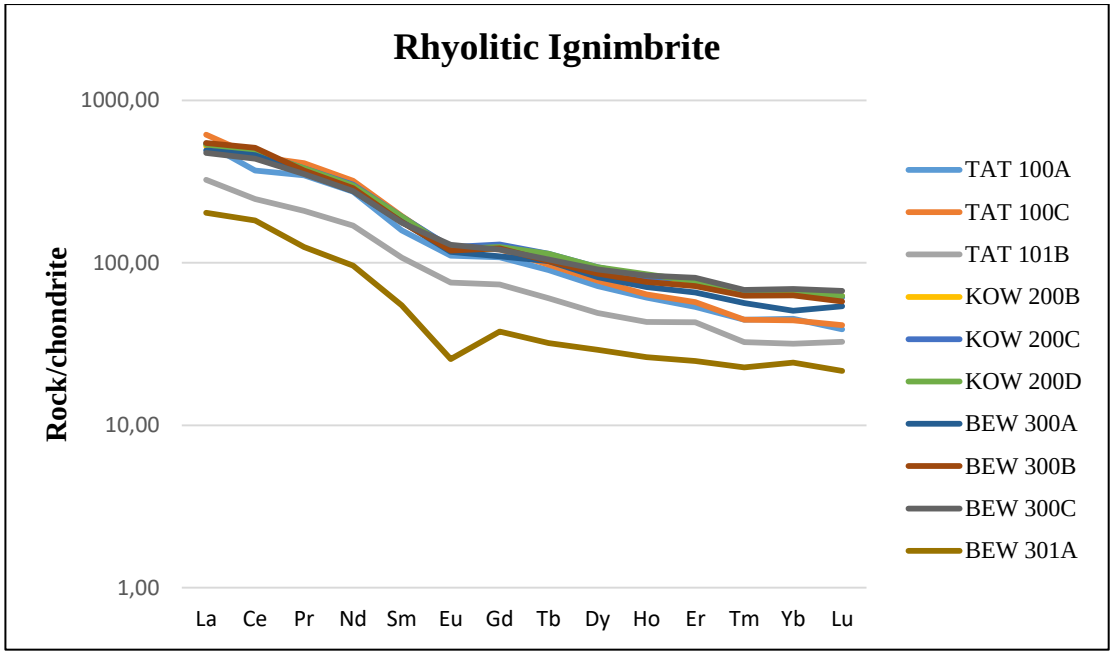

Figure 5.4: Chondrite-normalized REE diagram for rhyolitic ignimbrite.

5.3.2 Trace elements geochemistry of opal

The opal samples show typical depletion from LREE to HREE, However, a progressive increase from Gd to Lu. It is characterized by Eu negative anomaly, and a positive Ce anomaly (Fig. 5.5).

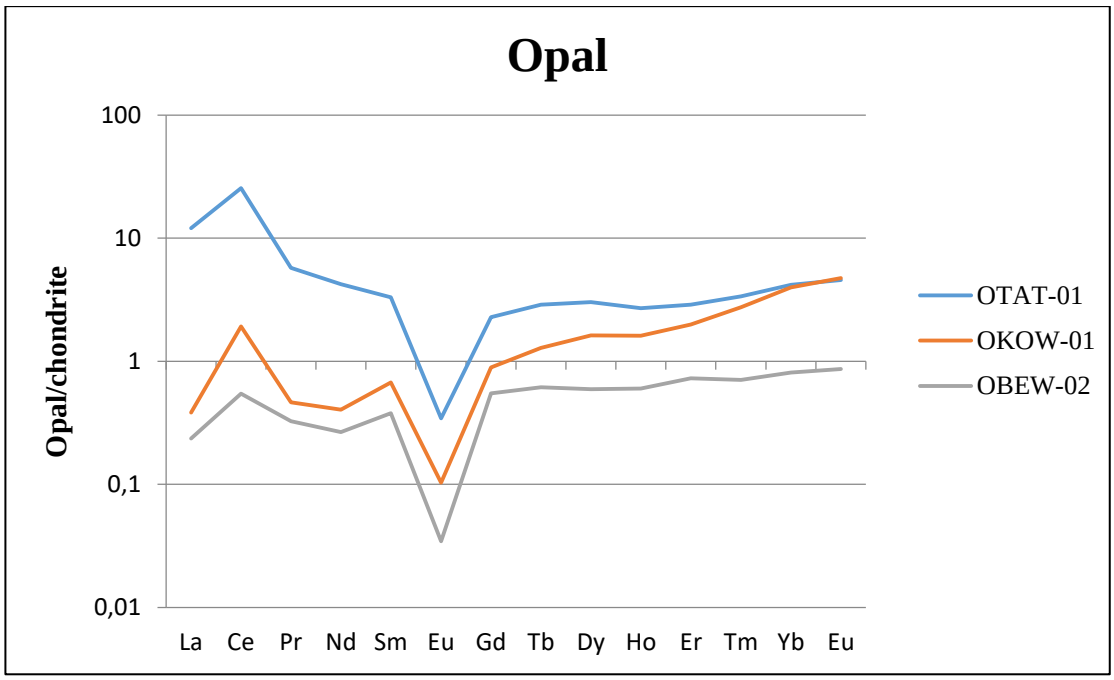

Figure 5.5: Chondrite-normalized REE diagram for opal samples.

The relationship between host rock and opal is shown in (Fig. 5.6). Their difference is the variation in concentrations between opal and its host rock with always a lesser element concentration in opal compared to its host rock, which can be attributed to a dilution. The anomalies (Eu and Ce) are observed in the opal which is absent in the host rhyolitic ignimbrite.

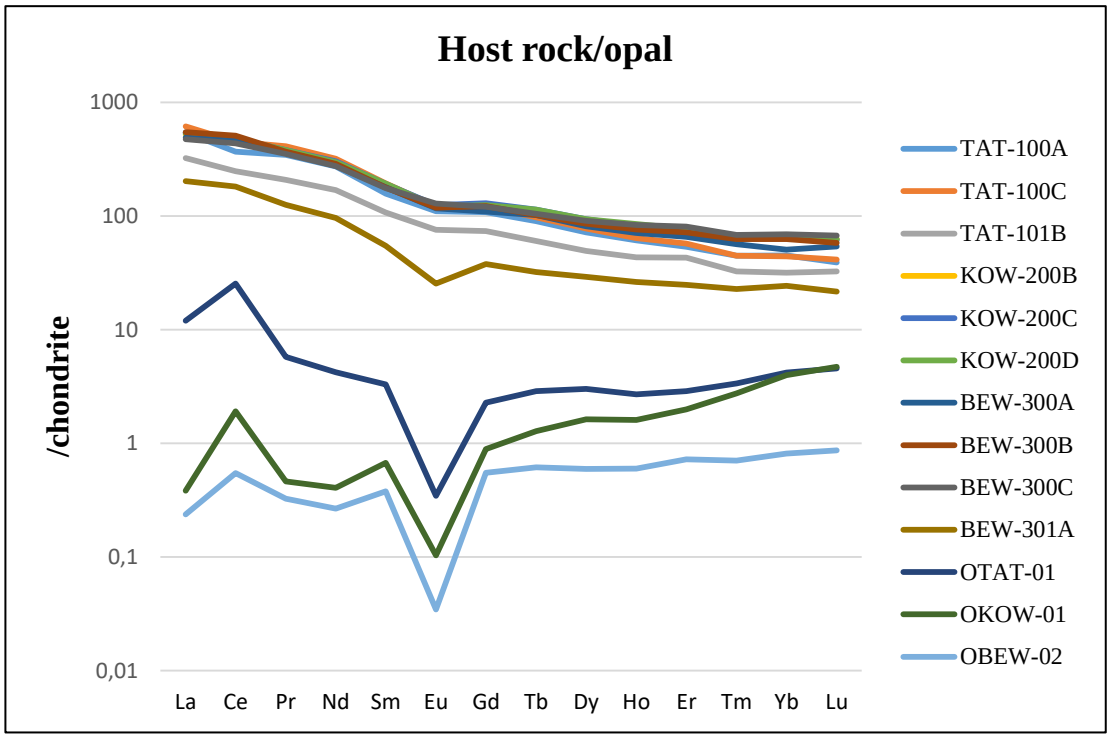

Figure 5.6: REE diagram of an opal compared to its host rock normalized to chondrite.

CHAPTER SIX

6. DISCUSSION

6. 1 INTRODUCTION

Gem quality opal occurs in one opal bearing horizon (Fig. 4.3, 6.1) ~3m thick within an unwelded, highly weathered rhyolitic ignimbrite bed. The bed is concordant with the layering and is characterized by brownish, friable soft rock, strongly weathered: altered volcanic glass, and granular microstructures cemented by opal. The beds have some difference in elevation due to the NW-SE oriented normal faults (Fig. 4.6). The interfaces between the overlying welded, and unweathered rhyolitic ignimbrite do not host the opal mineral. The same is true for the basalt that underlies the opal-bearing volcanoclastic rock unit.

Regarding the result of trace element geochemistry, rhyolitic ignimbrite and opal samples show variable characteristics always a lesser concentration in opal. The presence and concentration of trace elements in opals reflect primarily the host-rock composition, as silica in opal comes from its weathering. In addition, some of the differences might arise from weathering during opal precipitation (Gaillou et al. 2008).

The opal samples show a more or less pronounced enrichment in LREE compared to HREE, Eu negative anomaly, and generally a positive Ce anomaly. Whereas elsewhere in volcanic environments, opals have a negative Ce anomaly. This may indicate that during the formation of opals, conditions were oxidizing (Gaillou et al. 2008). However, the Ce anomaly was not present in the opal host rock, indicating that it comes from the weathering of the host rock. (Fig. 5.5). Negative Eu animaly might be Eu^{2+} is substituted by Ca^{2+} (Chauvire et al., 2019).

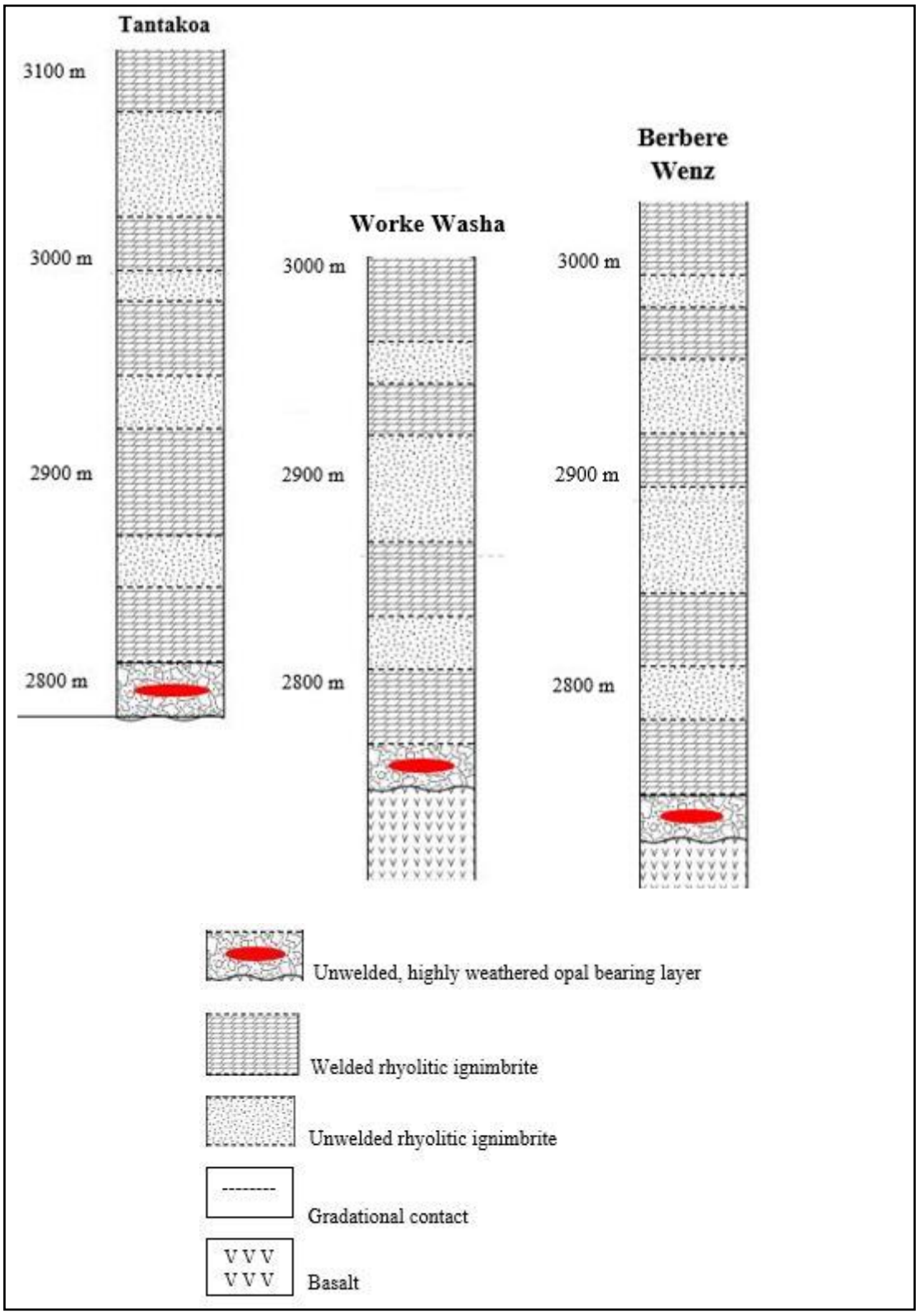

Figure 6.1: Log section of the investigated mining sites shows the stratigraphic position of the opal bearing layer and the other units of the area (no to scale). The elevation difference of opal bearing layer is due to normal fault.

6.2 DELANTA OPAL

Visually, most opals from the study area have a white body color, crystal opal, pale yellow to brownish red, and darker orange (fire opal). Rare samples have a dark brown body color (Fig. 6.2). The most common types of opal in the study area are described below.

White opal: - Precious opal with light body color, usually white, or cream with a play of color. It is also named as milky opal by local miners.

Fire opal: - is known for body-color of vivid orange or yellow. It typically shows no play of color or week play of color.

Crystal opal: - white to colorless, which has a transparent or semi-transparent body tone. It is found in many locations around the study area.

The mineralized layer extends for hundreds of meters and the excavations penetrate a 100–400 m underground tunnel into the mountain. The opal most often fills in fractures or cavities in the rock. As a result, the rough gem material has an irregular shape.

Figure 6.2: Polished play-of-color opals mined at Delanta, are white, brown to yellow, fire and show vivid play-of-color (polished by an individual on the study area).

6.3 COMPARISON WITH SOME KNOWN WORLD OPAL MINERAL

Opal has an infinite number of variables including color, pattern, brightness, and origin. However, there is currently no standardized method of grading opal though it is generally accepted that an opal from particular mining will fetch higher prices than similar-looking opal from elsewhere. This comparison is based on geochemistry and nature of opal to identify the geographic origin and quality respectively.

Delanta opal is one of the most diverse and spectacular types of opal on the market today (Rondeau et al., 2012). Australia has a worldwide reputation as the world's most expensive opals thus making opal the country's national gemstone (Liesegang and Milke, 2014; Dutkiewicz et al., 2013). Many countries now produce good opals like Mexico, Brazil, and USA. Each country's opals may be unique and this factor helps to determine the Opal price (Gaillou et al., 2008).

Color is the first thing that attracts people's aspirations. In order of value, the most valuable color is black, red, then orange, green, blue, and purple (Bobon, 2011). Most of the valuable color opals are originated from Australia and Mexico (Gaillou et al., 2008). Visually white, brown to yellowish (fire), and crystal opals are the most common in the study area. These opals are valued based on their vivid play of color (Fig. 6.2). The brighter and more intense the color, the higher the price of the opal. Australian and Brazilian opals are also characterized by the very vivid play of color. Unlike other opals, the Mexican opal does not usually exhibit a play of color. But it makes up for this with its remarkable body color (Gaillou et al., 2008).

Opals that have a rare or unique pattern (arrangement of colors) are more valuable. Most opals in Delanta have randomly arranged, anhedral and elongated patterns (Fig. 6.2). Wegel Tena opal have a naturally formed potch line with web inclusions known as the honeycomb pattern (Rondeau et al., 2010). This pattern is very rare in any other type of opals. These honeycomb shapes are also known on occasions to have a brighter or different color than the surrounding opal, this is also a rare occurrence in nature. The Harlequin pattern is the rarest and most loved pattern in opals but it is very rare and characteristics of some Australian opals (Dowell et al., 2003).

Wegel Tena opal can have ghost or phantom inclusions or vegetation matter (Rondeau et al., 2010). These types of inclusions are generally accepted as reasonable in this

type of opal. Opals from Australia also have the potential to showcase spectacular inclusion scenes, from pyrite crystals to black plumes of manganese oxide that stand out in high contrast to the play-of-color phenomenon. Other sources of natural opal that contain visually striking inclusions are Mexico and Brazil (Dutkiewicz et al., 2013).

Generally, volcanic-hosted opal (with exceptions, i.e. Mexican fire opal) is less stable than opal recovered from sedimentary rocks and often exhibits a greater propensity for crazing (Gaillou et al., 2008). A comparison of some world-known opal minerals from different literatures are summarized in table 6.1.

Table 6.1: Comparison between Delanta opal and some known world opal minerals.

Criteria	Delanta/Wegel Tena	Australia	Mexico	Brazil
Host rock	Rhyolitic ignimbrite	Sandstone and shale	Rhyolite and basalt	Sandstone
Type	CT	Both A & CT	CT	Both A & CT
Color	White, brown	White, black	Yellow,orange,orange-red	White, black
Direction/play of color	Very vivid, digit pattern	Very vivid	No/ rare	Very vivid
Pattern	Honeycomb	Harlequin	Pinfire	Dragonskin
Body tone	White,yellow,orange	Light,orange,black	Orange/ fire	White
Shape	Shield cut,heart,oval,free form	Round, oval	Round, oval	Oval,octagon,diamond
Inclusion	Phantom/vegetation matter	Pyrite, Manganese oxide	Quartz,geothite, rutile	Geothite, quartz
Opal field	South Wollo/ Delanta	Great Artesian Basin, Lightning Ridge	state of Queretaro, Hidalgo	Minas Gerais, Bahia, Rio Grande du Sul
Stability	Destabilization problem	Some Destabilization problem	Destabilization problem	Tougher than other opals

Based on geochemical singnature, REE diagrams of opals from volcanic and sedimentary environments show significant differences. Fig. 6.3, 6.4, and 6.5 presents typical examples of volcanic opals from Delanta compared to volcanic and sedimentary ones from Mexico and Brazil respectively. The REE patterns of volcanic opals show negative Eu anomaly inherited from the host rock. A positive Ce anomaly is present in Delanta opal REE patterns (Fig. 6.3). This anomaly is not present in the host rock (Fig. 5.4), which means that it comes during weathering. The transformation of Ce^{3+} into Ce^{4+} occurs under oxidizing conditions, giving a positive anomaly (Gaillou et al., 2008). REE patterns of sedimentary opals have weak to no Eu anomaly, and no Ce anomaly (Fig. 6.4 and 6.5).

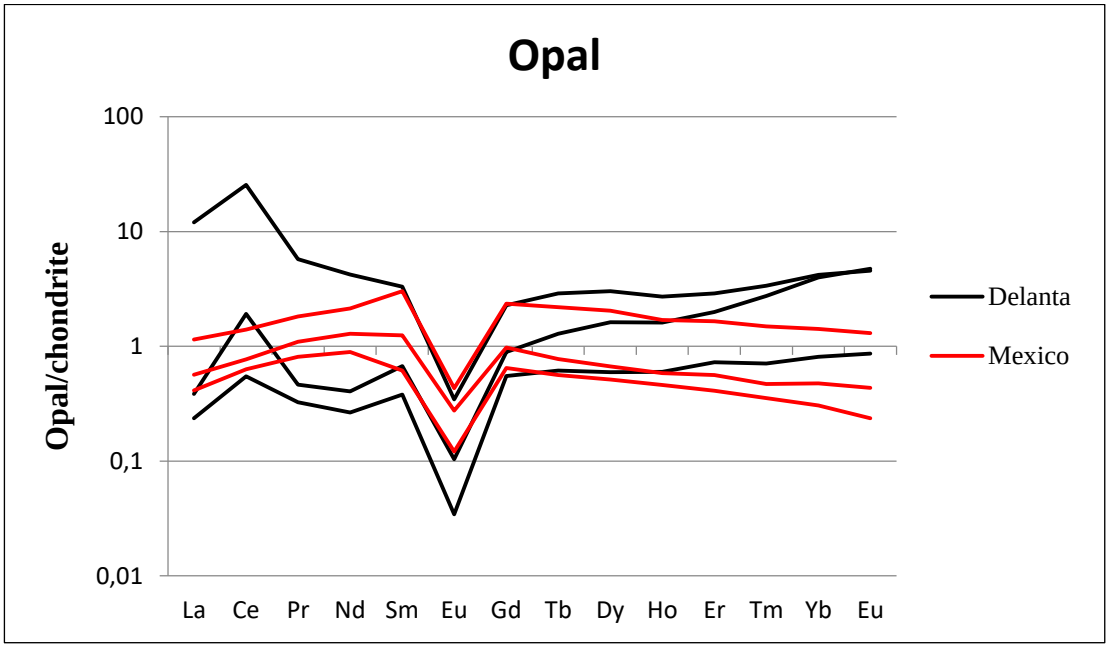

Figure 6.3: Chondrite-normalized rare earth element diagram of opal from Delanta/Mexico.

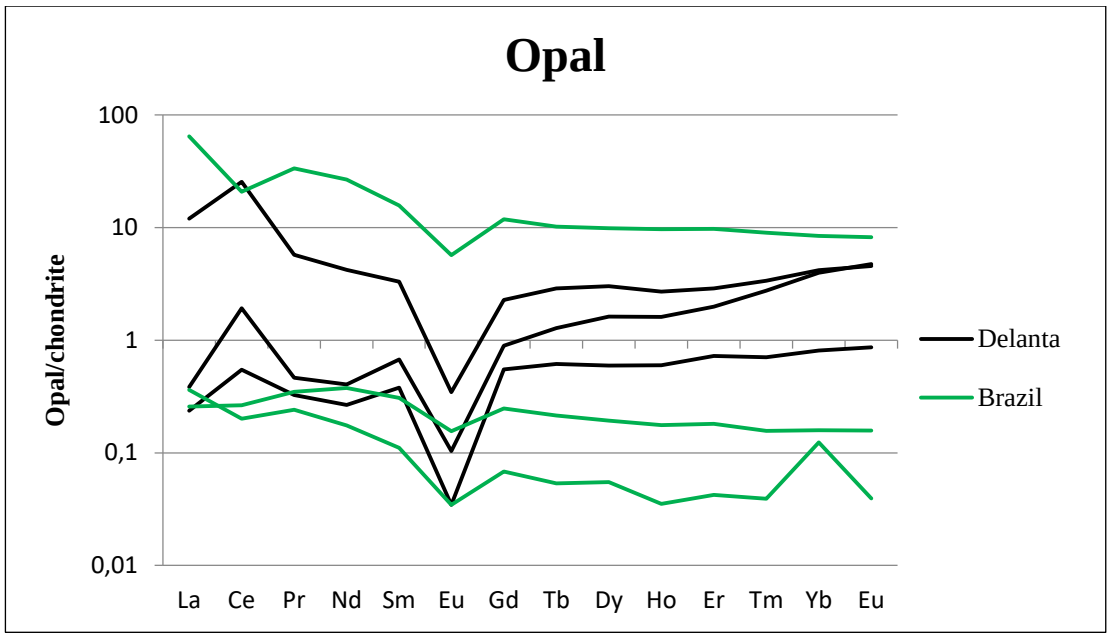

Figure 6.4**:** Chondrite-normalized rare earth element diagram of opal from Delanta/Brazil.

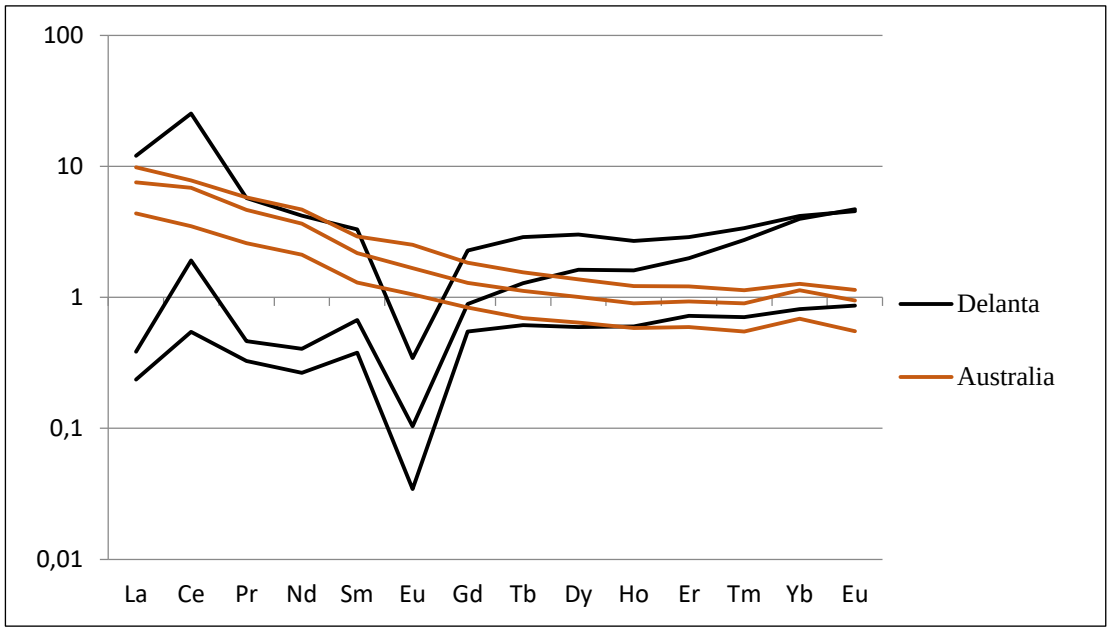

Figure 6.5**:** Chondrite-normalized rare earth element diagram of opal from Delanta/Australia.

When considering the comparison of the geochemical signature of opal from various geological contexts (volcanic or sedimentary host rocks), we find that volcanic opals follow this fairly good correlation based on REE pattern (Fig. 6.3). A significant variation [weak (Brazil) or absence (Australia) of Eu and generally no Ce anomaly] is seen in sedimentary opals (Fig. 6.4 and 6.5). This may suggest that controlling factors

of trace elements incorporation were different in volcanic and sedimentary environment.

The light rare earth element (LREE) - heavy rare earth element (HREE) ratio is higher in host rock than opal in Delanta. For example, in sample OKOW-01, La/Yb=0.14 for opal and =11.27 for the rhyolitic ignimbrite. This is explained by the proximity of the opal mineralization to the host rock. The LREE-HREE ratio is higher in opal than its host rock in Mexico. For example La/Yb=23 for opal and =2.3 for the rhyolite (Gaillou et al., 2008), meaning that HREE are more fractionated in the opal and they are known to be more incompatible than LREE, and so stay preferentially in the host rock (Gaillou et al., 2008). HREE are also less concentrated in the opal than in the Brazilian sandstone: La/Yb=19 in opal and 8 in the sandstone (Gaillou et al., 2008). This suggests that the HREE were stay in the host rocks and the fluid responsible for the formation of opal in Mexico and Brazil carried the silca and the mobile elements from the host rock and deposited away from the source.

Opals coming from very different deposits can look very much alike in color, or play of color. This makes the determination of opal's geographical origin uneasy. The geochemical criteria i.e. LREE-HREE ratio may help in determining the geographical origin. REE patterns are also strong indications of the geologic environment of opals.

6.4 GENESIS OF DELANTA OPAL

Opal forms either in volcanic or sedimentary deposits. It is believed to come from the weathering of silicic rocks (rhyolite or sandstones for example), followed by precipitation from a SiO_2-enriched liquid in cavities (Gaillou et al., 2008). Its deposition often occurs with rounded voids in rocks known as vesicles. Primary silicate minerals such as feldspars and feldspathoids and ferromagnesian minerals like pyroxene and hornblende are common parent materials that can cause the release of silica through their alteration by weathering or hydrothermal processes. Silica released in water precipitates in the form of quartz, chalcedony, or opal (Gaillou et al., 2008).

Strongly weathered opal-bearing horizon is characterized by: the presence of abundant clays, altered volcanic glass, and the granular microstructures are cemented by opal. The layer shows high LOI values (10.65-14.85 wt.%), that indicates the host rhyolitic ignimbrite were affected by weathering. Additionally, the opal samples show

a positive Ce anomaly which is absent in the host rock. This anomaly is the result of weathering of the host rock in oxidizing condition.

Based on these factors, it is proposed that, first rhyolitic ignimbrites were deposited. Then the deposition of Delanta opal were as surface or groundwater picks up silica from the products of the weathering processes of the host rhyolitic ignimbrite, forming silica solution and precipitated in primary and secondary openings like cracks, voids, openings, veins, which are caused by natural faults, fractures, decomposing fossils, and other silica deposit. These clearly demonstrates that Delanta opals formed during weathering of the host rhyolitic ignimbrite.

CHAPTER SEVEN

7. CONCLUSIONS AND RECOMMENDATIONS

7.1 CONCLUSIONS

- Delanta opal is mostly located around Wegel Tena, and Tsehay Mewucha locality. It has great importance in the country's economy and is now sold as raw materials or as cut and polished in the gemstone markets.
- During the fieldwork, in the three investigated mines, gem opal occurs in one lens-shaped opal bearing horizon within an unwelded and weathered rhyolitic ignimbrite bed and is composed of brownish, clayey, and soft friable rock. These mines are all located on the steep sides of the plateau, where the opal-bearing horizons outcrop. The later deposited cliff-forming welded, unweathered rhyolitic ignimbrite, that overlies the opal-bearing unit, can be used as an impermeable medium and used as a barrier for the storage of certain amounts of water and silica solution within the rhyolitic ignimbrite. Therefore, it may not be in a favorable condition for the weathering processes that may act upon it.
- The weathered condition (rich in clay) of the opal host rock indicates that the water may be from the surface or ground, responsible for the liberation of feldspar and volcanic glass from the host rock. It forms a solution and creates a favorable condition for the precipitation of opal in primary or secondary openings like cracks, voids, and openings.
- The result from petrographic examination shows similar petrography at all investigated sites. This might indicate the intensity of weathering was near similar in the study area.
- Elsewhere in volcanic environments, opals have a negative Ce anomaly. But Delanta opal is characterized by a positive Ce anomaly. This may indicate that during the formation of opals, conditions were oxidizing. However, the Ce anomaly was not present in the opal host rock, indicating that it developed during weathering. Substitution of Eu^{2+} by Ca^{2+} results negative Eu anomaly.
- Based on this investigation, (i.e. field observation, petrographic and geochemical analysis) strongly weathered opal-bearing horizon with the presence of abundant clays, altered volcanic glass, granular microstructure, high LOI values, and a positive Ce anomaly demonstrates that the studied opals formed during an episode of weathering of the host rhyolitic ignimbrite.

- When considering the comparison of the geochemical signature, based on LREE – HREE ratio (La/Yb), Delanta host rock is higher than the opal. But the La/Yb ratio is higher in opal than its host rock in Mexican and Brazil. La/Yb ratio can therefore often be useful in combination with other criteria to determine the geographical origin of an opal.

7.2 RECOMMENDATIONS

- This study focuses on whole-rock geochemistry (major and trace elements analysis) of the opal bearing layer only. There are other layers similar properties with opal bearing layer which are characterized by unwelded, and slightly weathered but do not accommodate opal. So it needs to investigate, why opal was not precipitated in these layers.
- To understand the temperature of formation and fluid composition of the opal bearing layer, oxygen isotope geochemistry should be carried out.

REFERENCES

Abbate, E., Bruni, P., and Sagri, M. (2015). Geology of Ethiopia: a review and geomorphological perspectives. *Landscapes and Landforms of Ethiopia*, 33-64.

Aguilar-Reyes, B.O. (2004). Microstructural study of opal: application to the destabilization by whitening. Ph.D. dissertation, University of Nantes.

Andrews, J. E., Brimblecombe, P., Jickells, T. D., and Liss, P. S. (1996). An introduction to Environmental Chemistry, School of Environmental Sciences, University of East Anglia.

Ayalew, D., Ebinger, C., Bourdon, E., Yirgu, G., and Grassineau, N. (2006). Temporal compositional variation of syn-rift rhyolites along the western margin of the southern Red Sea and northern Main Ethiopian Rift. *Geological Society Special Publication,* 259(1), 121-130.

Ayalew, D. and Yirgu, G. (2003). Crustal contribution to the genesis of Ethiopian plateau rhyolitic ignimbrites: basalt and rhyolite geochemical provinciality. *Journal of the Geological Society, London*,160, 47-56.

Barreto, S. B., and Bittar, S. M. (2010). The gemstone deposits of Brazil: occurrences, production, and economic impact. *Boletin de la sociedad geologica Mexicana,* 62(1), 123- 140.

Beccaluva, L., Bianchini, G., Natali, C., and Siena, F. (2009). Continental Flood Basalts and Mantle Plumes: a Case Study of the Northern Ethiopian Plateau. *Journal of* Petrology, 50 (7), 1377-1403.

Berhe, S. M., Desta, B., Nicoletti, M., and Teferra, M. (1987). Geology, geochronology, and geodynamic implications of the Cenozoic magmatic province in W and SE Ethiopia. *Journal of Geological Society,* 144(2), 213-226.

Bobon, M., Christy, A. A., Kluvanec, D., and Illánová, L. (2011). State of water molecules and silanol groups in opal minerals: a near-infrared spectroscopic study of opals from Slovakia. *Physics and Chemistry of Minerals*, *38*(10), 809-818.

Chamard-Bois, S. (2015). Bleaching of fire opals by oxalic acid. Unpublished technical report, Laboratory of Planetology and Geodynamics of Nantes, France, 1-65.

Chauvire, B., Rondeau, B., Alexandre, A., Chamard-Bois, S., Carole La C., and Mazzero, F. (2019). Pedogenic origin of precious opals from Wegel Tena (Ethiopia): Evidence from trace elements and oxygen isotopes. *Applied Geochemistry*, *101*, 127-139.

Coenraads, R. R., and Zenil, A. R. (2006). Leopard opal: play-of-color opal in vesicular basalt from zimapán, hidalgo state, Mexico. *Gems & Gemology*, 42(4), 236–246.

Croll, I. C. H. (1950). The opal industry in Australia. *Mineral Economist*, Bulletin no. 17. Pp. 1-46.

Dagnachew, S. (2017). Geology and stability of opal from Wegel Tena area, Ethiopia. Unpublished MSc Thesis, Addis Ababa University, Addis Ababa, Ethiopia.

Davies, M., Parkinson, I., and Rogers, N. (2003). The Origin of High-Ti Picrites from the Ethiopian Flood Basalt Province. In *Penrose Conference, Plume IV: Beyond the Plume Hypothesis, Tests of the plume paradigm and alternatives*.

Demissie, T., Yohannes, G., Mammo, A., Tesfaye, Y., Teshome, Y., Burusa, G., Edris, M., and Wenduante, M. (2010). Geology Geochemistry and gravity survey of the Dessie area. Ethiopian Institute of Geological Surveys, unpublished report, Addis Ababa.

Dowell, K., Mavrogenes, J., McPhail, D., and Chappell, J. (2003). Fantastic Australian opals.

Dutkiewicz, A., Landgrebe, T. C., and Rey, P. F. (2013). Origin of silica and fingerprinting of Australian sedimentary opals. *Gondwana Research*, *27*(2), 786-795.

Elzea, J. M., and Rice, S. B. (1996). TEM and X-ray diffraction evidence for cristobalite and tridymite stacking sequences in opal. *Clays and Clay Minerals*, 44(4), 492-500.

Filin, S.V., and Puzynin, A. l. (2009). Prevention of cracking in Ethiopian opal. *The Australian Gemmologist*, 23 (12), 579-582.

Fritsch, E., Rondeau, B., Ostrooumov, M., Lasnier, B., and Marie, A. M. (1999). Recent discoveries about opal. *Revue de Gemmology afg*, 138/139, 34-40.

Gaillou, E. (2006). Nanostructure Relations, Physical Properties and Formation Mode of Opals A and CT. Ph.D. dissertation, University of Nantes, France.

Gaillou, E., Delaunay, A., Rondeau, B., Bouhnik-le-Coz, M., Fritsch, E., Cornen, G., and Monnier,C. (2008). The geochemistry of gem opals as evidence of their origin. *Ore Geology Reviews*, 34 (1-2),113-126.

Gerra, S. (2000). A short introduction to the geology of Ethiopia, *Chronique de la Recherche minieral Na*, 540(2000), 3-10.

Guthrie, G. D., Dish, D. L., and Reynolds, R. C. (1995). Modeling the X-ray diffraction pattern of opal-CT. *American Mineralogist*, 80(7-8), 869-872.

Hofmann, C., Courtillot, V., Feraud, G., Rochette, P., Yirgu, G., Ketefo, E., and Pik, R. (1997). Timing of the Ethiopian flood basalt event and implications for plume birth and global change. *Nature*, 389(6653), 838–841.

Horton, D. (2002). Australian sedimentary opal: why is Australia unique. *The Australian Gemmologist*, 21 (8).

Iler, R. K. (1979). Silica in biology. *The chemistry of silica*, 1955, 730–801.

Johnson, M. L., Kammerling, R. C., DeGhionno, D. G., and Koivula, J. I. (1996). Opal from Shewa Province, Ethiopia. *Gems Gemmology*, *32(2)*, 112-120.

Jones, B., and Renaut, R.W. (2003). Hot spring and geyser sinters: the integrated product of precipitation, replacement, and deposition. *Canadian Journal of Earth Sciences*, 40(11), 1549–1569.

Jones, B., and Renaut, R.W. (2004). Water Content of Opal-A: implications for the origin of laminae in geyserite and sinter. *Journal of Sedimentary Research*, 74(1), 117–128.

Jones, J. T., and Segnit, E. R. (1971). The nature of opal I. Nomenclature and constituent phases. *Journal of the Geological Society of Australia*, 18(1), 57-68.

Kazmin, V. (1972). The Geology of Ethiopia Unpublished report, *EIGS*, Addis Ababa, Ethiopia.

Kiefert, L., Hardy, P., Sintayehu, T., Abate, B., and Woldetnsae, G. (2014). New Deposit of Black Opal from Ethiopia. *Gems & Gemmology*, 50(4).

Klein, C., Hurlbut, C.S., and JR. (1993) Manual of Mineralogy. John Wiley & Sons, *Inc., New York.*

Koivula, J. I., Fryer, C., and Keller, P.C. (1983). Opal from Queretaro, Mexico: occurrence and inclusions. *Gems & Gemmology*, 87-96.

Korme, T., Acocella, V., and Abebe, B. (2004). The Role of Pre-existing Structures in the Origin, Propagation, and Architecture of Faults in the Main Ethiopian Rift. *Gondwana Research*, 7(2), 467-479.

Liesegang, M., and Milke, R. (2014). Australian sedimentary opal-A and its associated minerals: Implications for natural silica sphere formation. *American Mineralogi*, 99(7), 1488–1499.

Merla, G. and Abbate, E. et al.(1979). A Geological Map of Ethiopia and Somalia (1973) and *Comment with a Map of Major Landforms. CNR*, Florence.

Mohr, P. (1983). Volcanotectonic aspects of the Ethiopian Rift evolution. *Bulletin Centre Recherches exploration-production Elf-Aquitaine*, 7(1), 175-189.

Mohr, P. A. (1962). The Geology of Ethiopia. *University. Coll of Addis Ababa press*. (reprinted in 1971 Haileselassie University press), Asmera, Ethiopia.

Mohr, P., and Zanettin, B. (1988). The Ethiopian flood basalt province. In Continental flood basalts. *Springer, Dordrecht*, 63-110.

Pik, R., Deniel, C., Coulon, C., Yirgu, G., Hofmann, C., and Ayalew, D. (1998).The northwestern Ethiopian Plateau flood basalts: classification and spatial distribution of magma types. *Journal of Volcanology and Geothermal Research*, 81(1-2), 91– 111.

Pik, R., Daniel, C., Coulon, C., Yirgu, G., and Marty, B. (1999). Isotopic and trace element signatures of Ethiopian flood basalts: Evidence for plume lithosphere interactions. *Geochemical Cosmochemica Acta*, 63(15), 2263-2279.

Pirajno, F. (2009). Hydrothermal processes and mineral system. *Springer Science and Business Media, Netherlands*.

Rondeau, B., Cenki-Tok, B., Fritsch, E., Mazzero, F., Gauthier, J. P., Bodeur, Y., Bekele, E., Gaillou, E., and Ayalew, D. (2012). Geochemical and petrological characterization of gem opals from Wegel Tena, Wollo, Ethiopia: opal formation in an Oligocene soil. *Geochemistry: Exploration, Environment, Analysis*, 12**(**2), 93-104.

Rondeau, B., Fritsch, E., Mazzero, F., and Gauthier, J. P.(2011). Opal- The Craze for Stability. *InColor, International Colored Gemstone Association*, 4, 2-5.

Rondeau, B., Fritsch, E., Mazzero, F., Gauthier, J. P., Cenki-Tok, B., Bekele, E., & Gaillou, E. (2010). Play-of-Color Opal from Wegel Tena, Wollo Province, Ethiopia. *Gems & Gemology*, *46*(2), 90-105.

Sanders, J.V. (1964). Colour of precious opal. *Nature*, 204(4964), 1151 – 1153.

Sun. S.S., and McDonough, W.F. (1989). Chemical and isotopic systematics of oceanic basalts: implications of mantle composition and processes. *Geological society, London, special publication*, 42(1), 313-345.

Wilson, M., and Guiraud, R. (1992). Magmatism and rifting in western and central Africa, Late Jurassic to Recent times. *Tectonophysics,* 213(1-2), 203-225.

Winchester, J.A. and Floyd, P.A. (1997). Geochemical discrimination of different magma series and their differentiation products using immobile elements. *Chemical Geology*, 20: 245-252.

Zewdie, S., Mammo, W., and Negassa, G. (2009).Opportunities for gem resource development in Ethiopia. Ethiopian Institute of Geological Surveys, unpublished report Addis Ababa.

ANNEX

Annex-A: List and location of rocks samples collected from the study area.

Sample				Description
No.	Code	Location		
1,	TAT-100A	0529172	1293271	Dark grey, gentle slope, aphanitic, unwelded, Rhyolitic Ignimbrite
2,	TAT-100B	0529172	1293271	Light grey, gentle slope, aphanitic, unwelded, Rhyolitic Ignimbrite
3,	TAT-100C	0529172	1293271	Dark and light grey in a common, gentle slope, aphanitic, unwelded, Rhyolitic Ignimbrite
4,	TAT-101B	0529123	1293261	Light grey, gentle slope, aphanitic, more welded, Rhyolitic Ignimbrite
5,	KOW-200A	0525552	1281697	Light grey, aphanitic, less welded, rock fragmented Rhyolitic Ignimbrite
6,	KOW-200B	0525552	1281697	Light grey, aphanitic, less welded, rock fragmented Rhyolitic Ignimbrite
7,	KOW-200C	0525552	1281697	Light grey, fine-grained, less welded Rhyolitic Ignimbrite
8,	KOW-200D	0525552	1281697	Light grey, fine-grained, less welded Rhyolitic Ignimbrite
9,	BEW-300A	0523966	1278623	Light to dark grey, aphanitic, unwelded, glass shards rhyolitic Ignimbrite
10,	BEW-300B	0523966	1278623	Light grey, aphanitic, unwelded, glass shards rhyolitic Ignimbrite
11,	BEW-300C	0523966	1278623	Dark grey, aphanitic, less welded, With opal inclusion, rock fragments Rhyolitic Ignimbrite
12,	BEW-300D	0523966	1278623	Light grey, fine-grained, rock fragment, unwelded Rhyolitic Ignimbrite
13,	BEW-301A	0523948	1278716	Light grey, more welded, fine to medium-grained, rock fragmented Rhyolitic Ignimbrite

Annex-B: Modal proportion and textures of the opal host rock.

Sample code	Rock		Modal proportion		Mineral form
	Name	Texture			
TAT-100A	Rhyolitic Ignimbrite	Vitrophric	Volcanic glass	80%	
			Quartz	8%	Anhedral
			Plagioclase	6%	Anhedral
			Biotite	2%	Anhedral
			Opaque minerals	2%	Anhedral
			Lithic fragments	2%	Anhedral
TAT-100B	Rhyolitic Ignimbrite	Vitrophric	Volcanic glass	80%	
			Quartz	7%	Anhedral
			Plagioclase	4%	Anhedral
			Sanidine	3%	Anhedral
			Biotite	3%	Anhedral
			Opaque minerals	1%	Anhedral
			Lithic fragments	2%	Anhedral
TAT-100C	Rhyolitic Ignimbrite	Vitrophric	Volcanic glass	85%	
			Plagioclase	8%	Anhedral
			Sanidine	4%	Anhedral
			Biotite	1%	Anhedral
			Opaque mineral	1%	Anhedral
			Lithic fragments	1%	Anhedral
TAT-101B	Rhyolitic Ignimbrite	Vitrophric	Volcanic glass	80%	
			Quartz	9%	Anhedral
			Plagioclase	6%	Anhedral
			Sanidine	3%	Anhedral
			Biotite	2%	Anhedral
			Opaque minerals	1%	Anhedral
			Lithic fragments	1%	Anhedral

Sample code	Rock		Modal proportion	Mineral form
	Name	Texture		
KOW-200A	Rhyolitic Ignimbrite	Vitrophric	Volcanic glass 85%	
			Quartz 7%	Anhedral
			Plagioclase 3%	Anhedral
			Sanidine 2%	Anhedral
			Biotite 1%	Anhedral
			Opaque minerals 1%	Anhedral
			Lithic fragments 1%	Anhedral
			Hornblende Trace	Anhedral
KOW-200B	Rhyolitic Ignimbrite	Vitrophric	Volcanic glass 82%	
			Quartz 7%	Anhedral
			Plagioclase 4%	Anhedral
			Biotite 2%	Anhedral
			Sanidine 2%	Anhedral
			Hornblende 1%	Anhedral
			Opaque minerals 1%	Anhedral
			Lithic fragments 1%	Anhedral
KOW-200C	Rhyolitic Ignimbrite	Vitrophric	Volcanic glass 85%	
			Quartz 6%	Anhedral
			Plagioclase 4%	Anhedral
			Hornblende 2%	Anhedral
			Opaque minerals 2%	Anhedral
			Lithic fragments 1%	Anhedral
KOW-200D	Rhyolitic Ignimbrite	Vitrophric	Volcanic glass 85%	
			Plagioclase 7%	Anhedral
			Quartz 4%	Anhedral
			Biotite 2%	Anhedral
			Opaque minerals 1%	Anhedral
			Lithic fragments 1%	Anhedral

Sample code	Rock		Modal proportion		Mineral form
	Name	Texture			
BEW-300A	Rhyolitic Ignimbrite	Vitrophyric	Volcanic glass	80%	
			Quartz	8%	Anhedral
			Plagioclase	5%	Anhedral
			Biotite	2%	Anhedral
			Sanidine	2%	Anhedral
			Opaque minerals	1%	Anhedral
			Lithic fragments	2%	Anhedral
BEW-300B	Rhyolitic Ignimbrite	Vitrophyric	Volcanic glass	78%	
			Quartz	7%	Anhedral
			Plagioclase	6%	Anhedral
			Sanidine	5%	Anhedral
			Biotite	2%	Anhedral
			Opaque minerals	1%	Anhedral
			Lithic fragments	1%	
BEW-300C	Rhyolitic Ignimbrite	Vitrophyric	Volcanic glass	80%	Anhedral
			Quartz	7%	Anhedral
			Plagioclase	6%	Anhedral
			Sanidine	5%	Anhedral
			Biotite	1%	Anhedral
			Lithic fragments	1%	Anhedral
BEW-300D	Rhyolitic Ignimbrite	Vitrophyric	Volcanic glass	78%	Anhedral
			Quartz	7%	Anhedral
			Plagioclase	7%	Anhedral
			Sanidine	5%	Anhedral
			Biotite	2%	Anhedral
			Lithic fragments	1%	Anhedral
BEW-301A	Rhyolitic Ignimbrite	Vitrophyric	Volcanic glass	80%	Anhedral
			Quartz	8%	Anhedral
			Plagioclase	6%	Anhedral
			Biotite	3%	Anhedral
			Sanidine	2%	Anhedral
			Lithic fragments	1%	Anhedral

Annex-C: Major elements analytical result of the host rock in wt. % (ICP-AES).

Sample No.	TAT-100A	TAT-100C	TAT-101B	KOW-200B	KOW-200C	KOW-200D	BEW-300A	BEW-300B	BEW-300C	BEW-301A
Rhyolitic Ignimbrite										
SiO2	57.8	56.8	58.7	59.5	59.8	59.9	58.6	56.6	56.2	64.6
Al2O3	13.25	13.75	13.50	13.45	14.00	13.75	14.20	14.50	14.05	13.25
Fe2O3	6.52	6.77	6.82	6.53	6.46	6.56	6.88	6.77	8.01	4.90
CaO	1.84	1.83	2.68	1.47	1.32	1.23	1.48	1.58	2.37	1.10
MgO	0.93	1.07	1.03	0.79	0.89	0.73	0.70	0.74	1.21	0.63
Na2O	1.25	1.17	1.39	1.76	2.07	2.08	1.50	1.27	2.11	1.83
K2O	1.55	1.39	1.75	1.94	1.74	1.85	1.75	1.53	1.44	2.72
TiO2	1.60	1.66	1.58	1.05	1.06	1.03	1.10	1.10	1.53	0.64
MnO	0.11	0.12	0.13	0.21	0.20	0.19	0.35	0.43	0.33	0.15
P2O5	0.08	0.08	0.52	0.09	0.11	0.11	0.05	0.05	0.23	0.01
LOI	14.40	14.85	13.05	13.15	11.80	12.10	13.65	14.55	11.90	10.65
Total	99.41	99.55	101.3	99.97	99.48	99.56	100.0	99.17	99.44	100.3

Annex-D: Trace element content (ppm) determined by ICP-MS (nd: not detected).

Sample no.			Ba	Ce	Cr	Cs	Dy	Er	Eu	Ga
TAT-100A	Trace Elements (ICP-MS) (ppm)	**Rhyolitic Ignimbrite**	598	226	20	2.63	18.25	8.88	6.42	30.2
TAT-100C			482	276	20	2.36	19.75	9.48	7.10	31.0
TAT-101B			511	151.5	20	2.52	12.50	7.14	4.38	29.4
KOW-200B			320	281	10	3.76	22.6	12.80	6.88	36.4
KOW-200C			293	295	10	3.62	23.9	13.10	7.24	39.6
KOW-200D			293	294	10	3.63	23.9	12.75	7.06	39.2
BEW-300A			366	282	10	3.84	20.7	10.85	6.79	42.8
BEW-300B			450	313	10	3.21	21.8	11.90	6.89	42.6
BEW-300C			403	268	20	2.25	23.1	13.40	7.49	40.0
BEW-301A			486	111.5	10	2.34	7.39	4.12	1.48	32.7
OTAT-01		**Opal**	18,39	15,555	nd	0,17	0,767	0,477	0,020	nd
OKOW-01			19,10	1,173	nd	0,23	0,412	0,329	0,006	nd
OBEW-02			31,88	0,333	nd	0,83	0,151	0,120	0,002	nd

Sample no.			Gd	Hf	Ho	La	Lu	Nb	Nd	Pr	Rb	Sm
TAT-100A	Trace Elements (ICP-MS) (ppm)	**Rhyolitic Ignimbrite**	22.2	14.1	3.45	129.0	0.99	71.2	128.0	32.9	67.7	24.2
TAT-100C			24.9	15.8	3.61	145.5	1.05	80.3	149.5	39.1	60.9	29.7
TAT-101B			15.15	14.1	2.45	76.8	0.83	71.2	79.3	19.80	76.0	16.45
KOW-200B			25.3	33.0	4.61	124.0	1.59	160.0	132.0	35.0	94.3	28.9
KOW-200C			26.7	35.7	4.62	128.0	1.56	174.0	141.5	36.3	85.9	29.4
KOW-200D			25.7	36.9	4.82	127.0	1.59	177.0	139.5	36.2	95.0	29.5
BEW3-00A			22.5	35.2	4.01	116.5	1.37	171.5	129.5	33.9	69.2	27.4
BEW-300B			25.2	37.7	4.32	129.5	1.47	183.5	134.5	35.1	63.6	27.3
BEW-300C			24.8	31.6	4.73	112.5	1.71	161.5	129.0	33.5	46.8	27.0
BEW-301A			7.75	13.7	1.49	48.1	0.55	62.7	44.9	11.90	89.3	8.37
OTAT-01		**Opal**	0,468	nd	0,153	2,852	0,116	15,82	1,969	0,546	2,81	0,505
OKOW-01			0,183	nd	0,091	0,091	0,120	22,49	0,189	0,044	5,94	0,103
OBEW-02			0,113	nd	0,034	0,056	0,022	2,05	0,124	0,031	17,28	0,058

Sample no.			Sn	Sr	Ta	Tb	Th	Tm	U	V	Y	Yb	Zr
TAT-100A	Trace Elements (ICP-MS) (ppm)	**Rhyolitic Ignimbrite**	5	219	4.4	3.37	9.32	1.14	5.03	59	82.3	7.68	573
TAT-100C			6	204	4.8	3.65	10.0	1.14	4.44	68	85.0	7.52	654
TAT-101B			5	265	4.1	2.26	9.38	0.83	2.44	71	74.8	5.40	587
KOW-200B			11	98.8	10.4	4.01	23.1	1.67	6.32	41	1135	11.0	1380
KOW-200C			12	82.4	11.2	4.26	24.9	1.67	6.39	69	1140	11.5	1450
KOW-200D			11	77.1	10.8	4.26	25.2	1.64	6.45	36	1160	11.0	1460
BEW-300A			11	88.6	10.9	3.83	24.3	1.44	5.78	72	93.6	8.62	1430
BEW-300B			11	83.7	11.2	3.83	26.4	1.60	5.59	56	1080	10.0	1540
BEW-300C			11	229	9.4	3.92	21.7	1.74	6.36	99	1210	11.5	1310
BEW-301A			6	78.3	3.3	1.20	10.5	0.58	2.70	28	37.5	4.14	483
OTAT-01		**Opal**	nd	10,2	nd	0,18	2,09	0,04	4,21	nd	3,09	0,72	68,8
OKOW-01			nd	13,2	nd	0,08	0,17	0,00	3,56	nd	3,13	0,65	57,3
OBEW-02			nd	70,7	nd	0,02	0,20	0,07	0,13	nd	1,60	0,18	10,5